Chem. Rev. 1994, 94, 737-757 737

Copper–Dioxygen Complexes. Inorganic and Bioinorganic Perspectives

Nobumasa Kitajima* and Yoshihiko Moro-oka

Research Laboratory of Resources Utilization, Tokyo Institute of Technology, 4259 Nagatsuta, Midori-ku, Yohokama 227, Japan

Received August 24, 1993 (Revised Manuscript Received February 18, 1994)

Contents

I. Introduction

Copper is an important element in oxidation catalysts for laboratory and industrial use. Aerobic oxidation of 2,6-xylenol with copper(I) in the presence of a N-donor ligand such as an amine or pyridine produces a *p*-phenylene oxide polymer which is widely used as an engineering thermoplastic under the trade name PPO.[1]

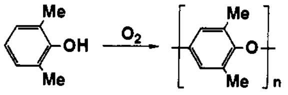

(eq 1)

Oxidation of ethylene to ethylene glycol is an important practical process, since ethylene glycol is a major intermediate for synthesis of polyesters and polyurethanes. Ethylene glycol is produced directly from ethylene by the Teijin process which utilizes a Cu/Br system as a catalyst.[2]

$$C_2H_4 + {}^1/_2O_2 + H_2O \rightarrow C_2H_4(OH)_2 \qquad \text{(eq 2)}$$

The synthesis of acetaldehyde by oxidation of ethylene, the so-called Wacker process, is a major process in the manufacture of organic chemicals starting from ethylene. The overall reaction is expressed in eq 3.

$$C_2H_4 + {}^1/_2O_2 \rightarrow CH_3CHO \qquad \text{(eq 3)}$$

Although palladium is the main catalytic component responsible for the production of acetaldehyde, copper is required as the most effective co-catalyst to re-oxidize Pd^0 to Pd^{2+} with molecular oxygen.[3]

The oxidative coupling of acetylenes to give diacetylenes is a well-known reaction catalyzed by copper, which is synthetically useful.[4] For example, many

$$2RC{\equiv}CR \xrightarrow{O_2} RC{\equiv}C{-}C{\equiv}CR \qquad \text{(eq 4)}$$

ethynyl compounds are coupled almost quantitatively by bubbling oxygen through an acetone solution of the acetylene in the presence of a copper(I) chloride–tetramethylethylenediamine complex.[4b]

Other oxidation reactions catalyzed by copper which are beneficial from a synthetic viewpoint include the following:[5,6]

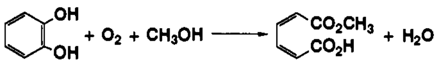

(eq 5)

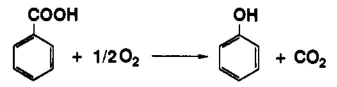

(eq 6)

Copper–dioxygen complexes are suggested to play important roles in these catalytic oxidation reactions, yet few such intermediates have been characterized, and the structural factors substantiating the catalytic effectiveness of the copper catalysts remain ambiguous. The oxidation chemistry of well-characterized copper–dioxygen complexes is, thus, expected to provide the basis for designing and developing new catalytic oxidation systems with copper as a main catalytic component.

Another primary interest in the copper–dioxygen complexes stems from the diverse occurrence of copper proteins which function as highly efficient biooxidation catalysts. In Table 1, the copper-containing proteins that bind or activate dioxygen are summarized. As can be seen, copper is an abundant element for proteins involved in dioxygen metabolism (exceeded probably only by iron), and a variety of physiological functions are known, dioxygen carrier, oxidase, oxygenase, and superoxide dismutase. Copper–dioxygen adducts are suggested as key reaction intermediates in these enzymatic reactions. The differentiation in the function of these proteins is attributed primarily to the coor-

0009-2665/94/0794-0737$14.00/0

Nobumasa Kitajima was born in 1954 in Tokyo. He received his B.S. degree in Chemical Engineering at the Tokyo Institute of Technology in 1977. He continued his research in the heterogeneous catalysis field directed by Professor Yoshio Ono at the Tokyo Institute of Technology and received his Ph.D. in 1982. He was a postdoctoral research associate working first with Professor Jeffrey Schwartz at Princeton University on surface organometallic chemistry from 1982 to 1984 and then with Professor Richard H. Holm on bioinorganic chemistry at Harvard University for one year. In 1985, he returned to Japan as an assistant professor at the Research Laboratory of Resources Utilization, Tokyo Institute of Technology, where since 1991 he has been an associate professor. His research interests include synthetic models for the active sites of metalloproteins, physical inorganic chemistry, catalysis of metalloenzymes and transition metal complexes, and roles of transition metal ions in biology.

Yoshihiko Moro-oka was born in 1938 in Ibaraki Prefecture of Japan. He received a B.S. degree in Applied Chemistry of Faculty of Engineering at the University of Tokyo in 1961. After a short experience in the chemical industry, he obtained his Ph.D. degree under the guidance of Professor Atsumu Ozaki at the Tokyo Institute of Technology in 1968. As a research associate at Research Laboratory of Resources Utilization, Tokyo Institute of Technology, he continued to study heterogeneous catalysis, especially catalysis by metal oxides. In 1975, he became an associate professor and he has been a professor of organic resources division since 1982. His research interests are directed to activation of dioxygen by heterogeneous and homogeneous catalysts, catalytic oxidations by metal oxides and organometallics, and preparation of key transition metal complexes to elucidate reaction mechanism of catalysis.

Table 1. Copper Proteins Involved in Dioxygen Metabolism

function	protein
dioxygen transport[a] $Hc + O_2 \rightleftarrows Hc\cdot O_2$	hemocyanin[b]
monooxygenation $X + O_2 + 2e^- + 2H^+ \rightarrow XO + H_2O$	tyrosinase[c] dopamine-β-monooxygenase[d] phenylalanine monooxygenase[e] peptidylglycine-α-amidating monooxygenase[f] methane monooxygenase[g] ammonia monooxygenase[h]
dioxygenation $X + O_2 \rightarrow XO_2$	quercetinase[i] 2,3-dihydroxybenzoate 2,3-dioxygenase[i] indole dioxygenase[i]
oxidation	
$O_2 + 4e^- + 4H^+ \rightarrow 2H_2O$	cytochrome *c* oxidase[j]
$2XH_2 + O_2 \rightarrow 2X + 2H_2O$	galactose oxidase[k]
$XH_2 + O_2 \rightarrow X + H_2O_2$	amine oxidase[l] ascorbate oxidase[m] laccase[n]
superoxide dismutation $2O_2^- + 2H^+ \rightarrow O_2 + H_2O_2$	Cu-Zn SOD[o]

[a] Hc denotes deoxyhemocyanin. [b] References 7–9. [c] Wilcox, D. E.; Porras, A. G.; Hwang, Y. T.; Lerch, K.; Winkler, M. E.; Solomon, E. I. *J. Am. Chem. Soc.* **1985**, *107*, 4015. [d] Stewant, L. C.; Klinman, J. P. *Ann. Rev. Biochem.* **1988**, *57*, 551. [e] Dix, T. A.; Benkovic, S. J. *Acc. Chem. Res.* **1988**, *21*, 101. [f] Eipper, B. A.; Perkins, S. N.; Hustein, E. J.; Johnson, R. C.; Keutmann, H. T.; Mains, R. E. *J. Biol. Chem.* **1991**, *266*, 7827. [g] Reference 121. [h] Hyman, M. R.; Arp, D. J. *J. Biol. Chem.* **1992**, *267*, 1534. [i] Keevil, T.; Mason, H. S. *Methods Enzymol.* **1978**, *52*, 3. [j] Reference 124. [k] Reference 120. [l] Reference 119. [m] Reference 123. [n] Reference 122. [o] Reference 129.

dination structure of the copper–dioxygen intermediate formed in the protein matrices, depending on the ligand donors, the geometry, and the coordination mode of the dioxygen. However, the correlation between these structural factors and the function/catalysis of the enzymes remains to be elucidated.

Among these copper proteins, hemocyanin, which is a widely occurring oxygen-transport protein for invertebrates, arthropods, and mollusks, forms a stable dioxygen adduct, so-called oxyhemocyanin. This adduct exhibits very unusual spectral properties,[7–15] which are reviewed in detail by Solomon in this issue. These characteristic spectral properties of oxyhemocyanin *have been suggested to reflect the unique coordination* mode of the peroxide at the dicopper site in hemocyanin, and the binding mode of the dioxygen in oxyhemocyanin has attracted the attention of many chemists. Accordingly, the synthesis and structural characterization of dinuclear μ-peroxo–copper(II) complexes which mimic the characteristic properties of oxyhemocyanin have been the focus of numerous recent and ongoing investigations.[16–21]

The versatile utility of copper as an oxidation catalyst, particularly in biological systems, indicates that formation of copper–dioxygen complexes is feasible, yet the isolation of such species is difficult, because of their extreme instability with conventional ligand systems, such as simple amines. The stability of copper–dioxygen complexes depends strongly on the ligands employed, as described below. Because of the thermal instability, earlier attempts to isolate and structurally characterize copper–dioxygen complexes were unsuccessful. Recent advancement in low-temperature spectroscopic techniques including UV–vis, resonance Raman, XAS, however, makes it possible to structurally identify the thermally unstable copper–dioxygen complexes. Moreover, the development of appropriate ligand systems has enabled the isolation and even crystallographic determination of the molecular structures of copper–dioxygen complexes.

In this article, we focus on the recent development of copper–dioxygen chemistry, mainly achieved since

1988. The work performed before that time was reviewed in detail in the article by Karlin et al.[20] which covers the literature before 1987. Several other reviews dealing with recent advances in copper–dioxygen chemistry have appeared.[16,17,21]

II. Reactions of Copper(I) Complexes with Dioxygen

Many factors affect the reactivity of copper(I) complexes toward dioxygen. Since the reaction causes one-electron oxidation of copper with reduction of dioxygen, the oxidation potential of Cu(I,II) couple is one of the important factors governing the reaction between the copper complex and dioxygen. The redox potentials of copper complexes vary dramatically depending upon the ligand environment due to the donor set, geometry, substituent electronic effect, substituent steric effect, and chelate size.[19b,20,22] The solvent gives a strong effect as well. Accordingly, a wide range of reduction potentials (−1.5 to +1.3 V vs NHE)[17] is known for copper complexes. For copper(I) complexes of positive reduction potential, one-electron reduction of dioxygen is a thermodynamically unfavorable process, since the E^0 is −0.33 V for $O_2 + e^- \rightarrow O_2^-$, while the four-electron or two-electron reduction of dioxygen to water or hydrogen peroxide are favorable reactions. Although the reduction potential is a good predictor of the reactivity of the copper(I) complex toward dioxygen, it is not directly correlated with the feasibility for the formation of the dioxygen adduct, since the redox potentials are defined for outer-sphere-type electron-transfer reactions.

The feasibility of formation of the dioxygen adduct is associated with both thermodynamic and kinetic factors. The former factor is directly related to the stability of the resultant dioxygen adduct. The ligand environment of the copper complex plays the crucial role for stability; the contributors to stability include again the ligand donor set, geometry, and substituent electronic and steric effects. The availability of an open coordination site to bind dioxygen and the steric bulk of the ligand substituent groups are also important, having a striking kinetic effect on the binding rate of dioxygen to the copper center. The role of solvent is of significance, since the availability of the open coordination site is dependent on the solvent, and the stability of the dioxygen adduct is influenced by the interaction between the dioxygen adduct and the solvent, e.g. hydrogen bonding and dipole interaction. Finally, factors which protect the dioxygen adduct from decomposition are of importance. In particular, the shielding effect of ligand substituent groups around the coordinated dioxygen is crucial to inhibit attack of a secondary copper ion or some other components (such as a proton) to cause the facile decomposition of the dioxygen adduct.

The total mix of these factors determines whether the reaction between a copper complex and dioxygen is facilitated or whether the dioxygen adduct is stable enough to be characterized or is even isolable. Since the overall effects are quite complex and beyond prediction, the design of suitable ligand systems and reaction conditions are not easy to accomplish. Accordingly, only a limited number of examples of well-characterized copper–dioxygen complexes have been reported so far.

III. Superoxo–Copper(II) Complexes

The redox potentials of a number of copper(I) complexes are low enough to reduce dioxygen to superoxide, and thus these complexes, if they are coordinatively unsaturated, are susceptible to dioxygen, and potentially it is possible to form a superoxo–copper(II) complex. In many cases, the superoxo–copper(II) complex reacts with another copper(I) ion readily, resulting in formation of a μ-peroxo dinuclear copper(II) complex. From a theoretical point of view, two-electron reduction of dioxygen with a copper(I) complex to generate a peroxo–copper(III) species is possible, but with the ligand systems known to date, the redox potential Cu(II,III) is not suitable for the formation of such a species. This type reaction step was proposed to occur in a biological system,[23] however, recent evaluation has provided negative evidence.[24] Consequently, a superoxo–copper(II) complex is an important initial reaction intermediate formed in copper–dioxygen chemistry in general. Nevertheless, its isolation has not been accomplished so far and only a very few examples of well-characterized superoxo–copper(II) complexes are known.

The first mononuclear superoxo–copper(II) complex was reported by Valentine et al.[25] Reaction of KO_2 with a N_4 macrocyclic copper(II) complex Cu(tet b)$^{2+}$ in DMSO gave a complex which exhibits a d–d band at 672 nm. The presence of the d–d band suggests that the formed complex is still cupric, yet the complex was EPR silent. This apparent diamagnetism is attributable to a strong magnetic coupling between the superoxide and the cupric ion, thus lending support to the assignment that the formed species is a superoxo–copper(II) complex. The CV data are also consistent with the structure. Formation of a superoxo complex from a monomeric copper(I) precursor was demonstrated by Thompson.[26] The reaction of a copper(I)–ethylene adduct $Cu(C_2H_4)[HB(3,5\text{-}Me_2pz)_3]$ with dioxygen gave $Cu(O_2)[HB(3,5\text{-}Me_2pz)_3]$ as a purple solid. The structural identification of the complex was based on its diamagnetism and IR spectral change with $^{18}O_2$ substitution. The complex exhibits an intense absorption band at 524 (600) [absorption band in nanometers (ϵ in cm^{-1} M^{-1}/Cu)], which was tentatively assigned to $O_2^- \rightarrow$ Cu(II) LMCT band. However, except the IR result, which was not credible [the $\nu(^{16}O-^{16}O)$ was not ascertained firmly], the properties of the complex are extremely similar to the μ-η^2:η^2-peroxo dinuclear copper(II) complex $[Cu[HB(3,5\text{-}Me_2pz)_3]]_2(O_2)$ which will be described in detail later, raising a debate as to whether the complex was misidentified. Treatment of a monomeric copper(I) complex with a tripodal tetradentate ligand [(TMPA)Cu(RCN)]$^+$ with dioxygen at −85 °C resulted in self-assembly, yielding a *trans*-μ-1,2-peroxo complex $\{[Cu(TMPA)]_2(O_2)\}^{2+}$ (vide infra). However, the initial reaction, explored carefully at −90 to −75 °C, indicated the formation of another complex that exhibits characteristic bands at 410 (4000) and 747 (1000).[27] In conjunction with dioxygen consumption quantitation and kinetic experiments, the formed species was proposed to be a monomeric superoxo complex. When a copper(I) precursor with BPQA in

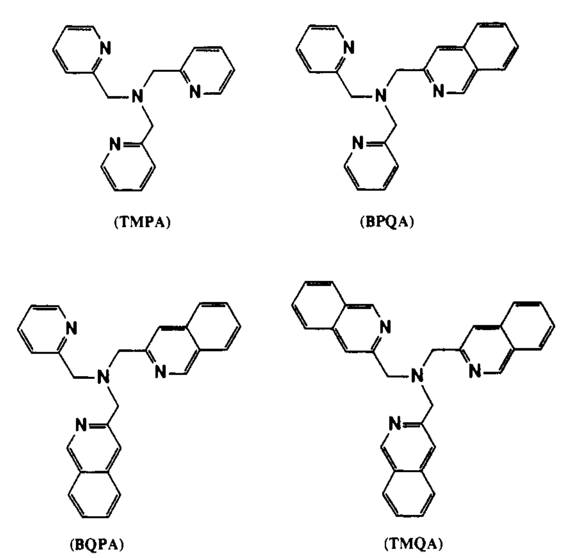

Figure 1. Tripodal tetradentate ligands used for synthesis of superoxo-copper(II) complexes.

which one of 2-pyridyl donors in TMPA was substituted with a 2-quinolyl group (see Figure 1) was treated with dioxygen at −80 °C, formation of a superoxo adduct was not observed and only a product obtained exhibited spectroscopic properties very similar to those of the *trans*-μ-1,2-peroxo complex $\{[Cu(TMPA)]_2(O_2)\}^{2+}$.[27b] While a copper(I) complex with TMQA is unreactive toward dioxygen presumably because of the highly steric bulk of the ligand due to substitution with three 2-quinolyl groups, the complex with BQPA containing two 2-quinolyl groups reacted with dioxygen. Thus, when the yellow solution of the copper(I) precursor with BQPA was oxygenated at −80 °C, an intense purple color solution was initially formed; this is ascribed to the generation of a *trans*-μ-1,2-peroxo complex $\{[Cu(BQPA)]_2(O_2)\}^{2+}$. However, this color quickly disappeared and transformed to a brown color solution which was stable at −80 °C. The manometric measurement indicated the ratio $Cu/O_2 = 1$, suggesting the formation of a superoxo complex $[(BQPA)Cu(O_2)]^+$, while its UV-vis features [378 (8200)] are considerably different from those of the superoxo adduct with TMPA. The superoxo complex with BQPA is thermodynamically more stable than the *trans*-μ-1,2-peroxo complex, whereas with TMPA the *trans*-μ-1,2-peroxo complex is more stable. This may be associated with the more steric hindrance of BQPA than TMPA, and the initial formation of the μ-peroxo complex was explained in terms of the kinetic "overshooting".[27b] Very recently, a superoxo dinuclear copper(II,II) complex has been reported.[28] A dinuclear copper(I) complex with an unsymmetric dinucleating ligand (designated as UN-O^- whose structure is given in Figure 7) reacts with dioxygen reversibly to afford a terminal peroxo dinuclear copper(II,II) complex (the details will be described later). One-electron oxidation of the peroxo complex with Ag^+ yielded a novel superoxo dinuclear copper(II,II) complex. The same complex was obtained by direct dioxygen addition to a mixed-valence copper(I,II) complex with the same ligand which was derived from the copper(I,I) complex by one-electron oxidation. The complex exhibits a characteristic band at 404 (5400) which is tentatively assignable to $O_2^- \rightarrow Cu(II)$ LMCT band. In none of the systems described above, direct evidence for the superoxo structure, such as the resonance Raman spectrum or X-ray crystallography, has been provided yet. Clearly, more extensive investigations on superoxo copper(II) complexes must be undertaken in the near future.

IV. Peroxo-Dinuclear Copper(II) Complexes

A. *Trans*-μ-Peroxo Complexes

The self-assembly of a monomeric copper(I) precursor with TMPA in the presence of dioxygen at low temperature (below −80 °C) afforded a thermally unstable *trans*-μ-1,2 peroxo complex $\{[Cu(TMPA)]_2(O_2)\}^{2+}$. As described already, the initial intermediate formed in this reaction is formulated as a monomeric superoxo complex, which was characterized by low-temperature UV-vis spectroscopy. The subsequent reaction of the putative superoxo complex with a copper(I) precursor results in the formation of the *trans*-μ-1,2-peroxo complex as follows:

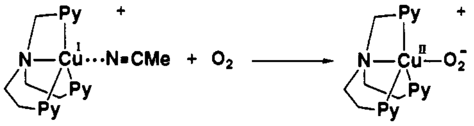

(eq 7)

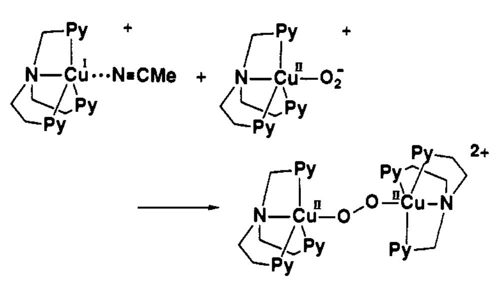

(eq 8)

The structure of $\{[Cu(TMPA)]_2(O_2)]^{2+}$ was determined by X-ray crystallography.[29] The ORTEP view of the μ-peroxo complex is presented in Figure 2. The molecule sits on a crystallographic inversion center of symmetry. The O–O bond length of 1.43 Å is typical for a peroxide ion coordinated to a transition metal ion.[15] The coordination environment of the copper is best described as distorted trigonal bipyramidal; one oxygen atom from the peroxide and the amine nitrogen serve as axial ligands. Hence, the unpaired electron of the cupric ion lies in the d_{z^2} orbital which is oriented along the Cu–O bond. Accordingly, a strong magnetic coupling between the two cupric ions through the peroxide ion is anticipated. In fact, $-2J$ estimated on the basis of variable-temperature magnetic susceptibilities of $\{[Cu(TMPA)]_2(O_2)\}^{2+}$ is as much as 700 cm^{-1}.[30] SCF-Xα-SW calculations performed for a model $\{[Cu(NH_3)_4]_2(O_2)\}^{2+}$ with an idealized trigonal-bipyramidal coordination environment indicated a moderately strong antiferromagnetic coupling of $-2J = 500$ cm^{-1}.[31] $\{[Cu(TMPA)]_2(O_2)\}^{2+}$ exhibits three characteristic absorption bands at 435 (1700), 524 (11 300), and 615 (5800). On the basis of the resonance Raman profile experiments in conjunction with SCF-Xα-SW calculations,[31] these three bands were assigned to peroxide-to-copper charge-transfer bands due to the spin-forbidden triplet transition from π^*_v, the electronic dipole-allowed singlet transitions from π^*_σ and π^*_v, respectively. This assignment is based on their energy ordering and relative intensities. Thus, the higher

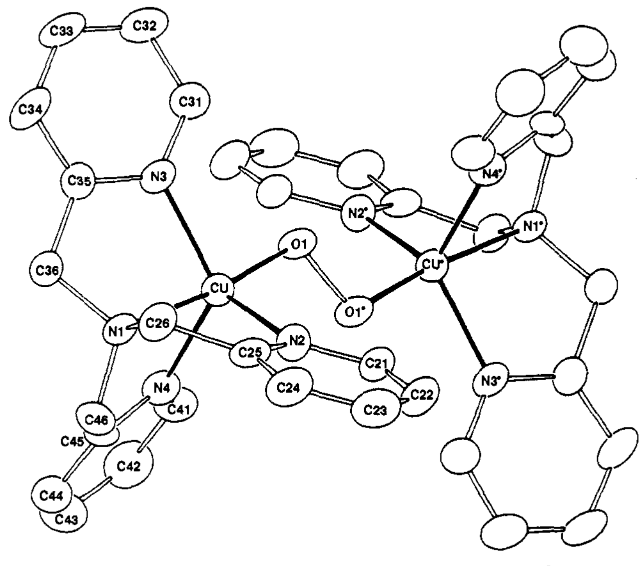

Figure 2. ORTEP view of $\{[Cu(TMPA)]_2(O_2)\}^{2+}$. The selected bond distances (Å) and angles (°) are as follows: Cu···Cu, 4.359(1); O1–O1′, 1.432(6); Cu–O1, 1.852(5); Cu–N1, 2.104(6); Cu–N2, 2.102(6); Cu–N3, 2.204(7); Cu–N4, 2.082(7); O1–Cu–N1, 173.7(3); Cu–O1–O1′, 107.7(2). (Reprinted from ref 29a. Copyright 1988 American Chemical Society.)

energy and more intense bands are assigned to the spin-allowed transitions, whereas the resonance enhancement profile of ν_s(Cu–O) (561 cm^{-1}) endorses the assignment of the 435-nm band.[31]

B. μ-η^2:η^2-Peroxo Complexes

Oxidation of a copper(I) complex $Cu(PPh_3)[HB(3,5\text{-}Me_2pz)_3]$ with PhIO afforded a μ-oxo dinuclear copper(II) complex $[Cu[HB(3,5\text{-}Me_2pz)_3]]_2O$.[32a] The putative structure was identified on the basis of the spectroscopic analysis including FD-MS and its effectiveness toward several oxo-transfer reactions. When the μ-oxo complex was treated with H_2O_2, a novel μ-peroxo dinuclear copper(II) complex was formed as shown in eq 9.[32b,c]

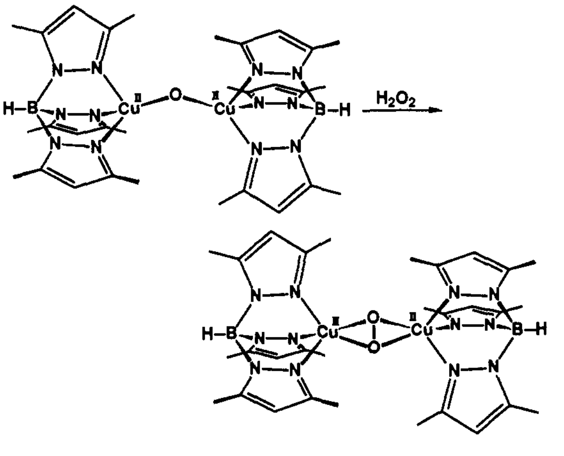

(eq 9)

This complex bears many similarities to those of oxyhemocyanin in its magnetic, electronic, and Raman spectra as described in detail below. While the X-ray structure was not determined, the FD-MS analysis supported a dinuclear structure bridged solely by a peroxide and thus it is formulated as $[Cu[HB(3,5\text{-}Me_2pz)_3]]_2(O_2)$. Subsequently, with two other more hindered hydrotris(pyrazolyl)borate ligands employed to enhance the stability and crystallinity, analogous μ-peroxo complexes $[Cu[HB(3,5\text{-}Ph_2pz)_3]]_2(O_2)$ and $[Cu[HB(3,5\text{-}iPr_2pz)_3]]_2(O_2)$ were prepared either by direct dioxygen addition to a monomeric copper(I) precursor $Cu(Me_2CO)[HB(3,5\text{-}Ph_2pz)_3]$ or $Cu[HB(3,5\text{-}iPr_2pz)_3]$ and by H_2O_2 treatment of a bis(μ-hydroxo) dinuclear copper(II) complex $[Cu[HB(3,5\text{-}iPr_2pz)_3]]_2(OH)_2$ as shown in eqs 10 and 11, respectively.[33]

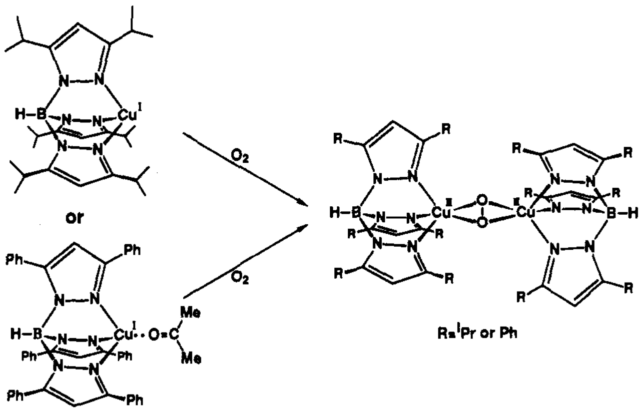

(eq 10)

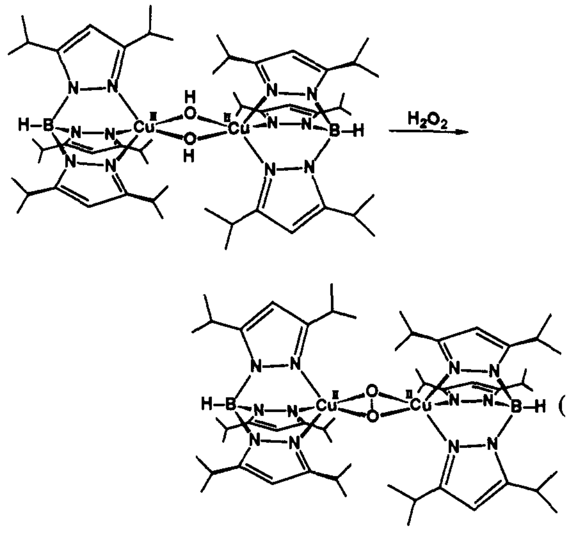

(eq 11)

Slow recrystallization of $[Cu[HB(3,5\text{-}iPr_2pz)_3]]_2(O_2)$ from CH_2Cl_2 at low temperature gave solvated crystals $[Cu[HB(3,5\text{-}iPr_2pz)_3]]_2(O_2)\cdot6(CH_2Cl_2)$ suitable for X-ray diffractions. Whereas the quality of the data collected was not excellent because of the facile loss of solvent of crystallization, the X-ray structure of $[Cu[HB(3,5\text{-}iPr_2pz)_3]]_2(O_2)\cdot6(CH_2Cl_2)$ definitely established the novel coordination mode of the peroxide referred to as a planar μ-η^2:η^2.[33] The perspective view of the molecule $[Cu[HB(3,5\text{-}iPr_2pz)_3]]_2(O_2)$ is presented in Figure 3. The molecule sits on a crystallographically imposed center of symmetry. Thus, the two cupric ions and the peroxide ion define a plane; two of the pyrazole nitrogens N11 and N31 are tightly bound to each copper and are close to the dicopper–peroxo plane as evidenced in the expanded view of the $N_3Cu(O_2)CuN_3$ moiety given in Figure 4. The other Cu–N (N21) bond distance is distinctly elongated. Hence, the coordination geometry of the copper is best described as square pyramidal with N21 as an apical ligand, although it is very distorted. The Cu···Cu separation of $[Cu[HB(3,5\text{-}iPr_2pz)_3]]_2(O_2)$ is 3.56 Å, which is considerably shorter than that found in the *trans*-μ-1,2-peroxo dinuclear copper-

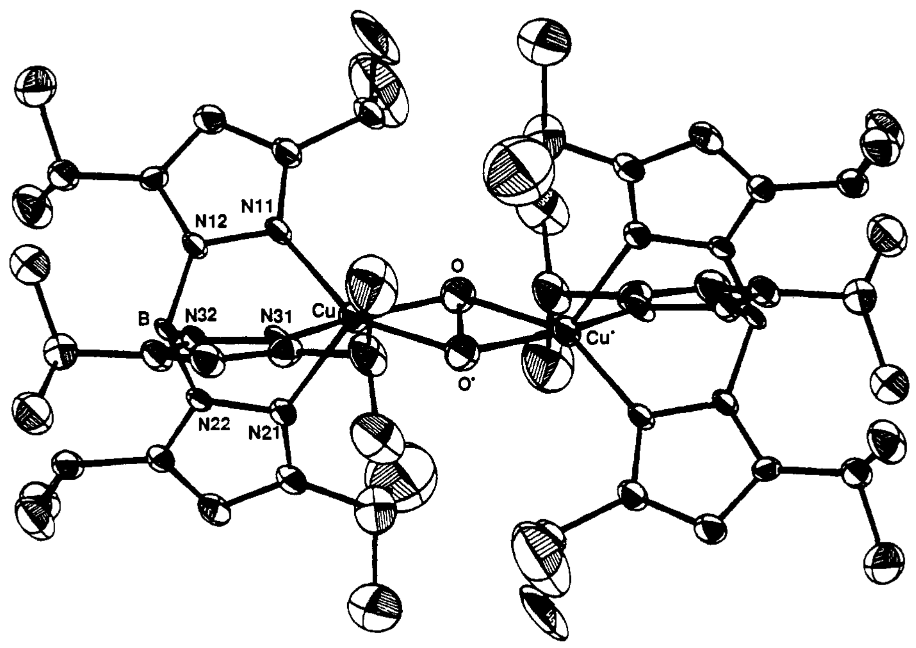

Figure 3. ORTEP view of $[Cu(HB(3,5\text{-}iPr_2pz)_3)]_2(O_2)$. (Reprinted from ref 33b. Copyright 1992 American Chemical Society.)

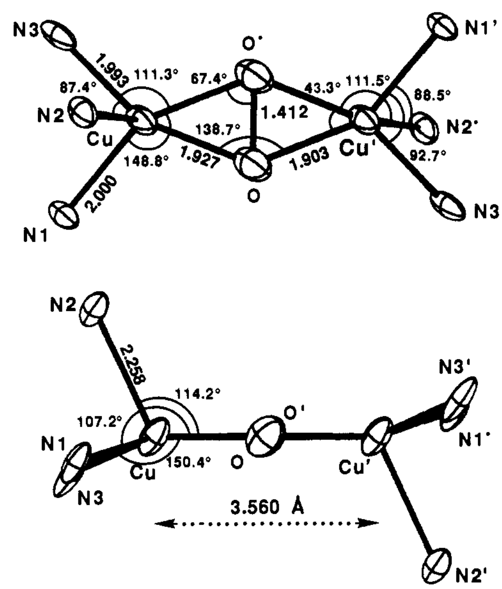

Figure 4. Expanded view of the $N_3Cu(O_2)CuN_3$ moiety in $[Cu[HB(3,5\text{-}iPr_2pz)_3]]_2(O_2)$.

(II) complex $\{[Cu(TMPA)]_2(O_2)\}^{2+}$ (4.36 Å).[29]

Two examples of planar μ-η^2:η^2-peroxo complexes of La[34] and U[35] are known and very recently a bent μ-η^2:η^2 coordination mode of the peroxide was found in a V complex.[36] The driving force for the unusual coordination modes in these complexes is reasonably attributable to the high oxophilicity of these elements. However, this interpretation cannot be applied to $[Cu[HB(3,5\text{-}iPr_2pz)_3]]_2(O_2)$, since cupric ion is not particularly oxophilic. Rather, it seems more likely that the μ-η^2:η^2 structure found in $[Cu[HB(3,5\text{-}iPr_2pz)_3]]_2(O_2)$ [or $[Cu[HB(3,5\text{-}Me_2pz)_3]]_2(O_2)$ and $[Cu[HB(3,5\text{-}Ph_2pz)_3]]_2(O_2)$] is associated with the strong peculiarity of cupric ion to favor a square-pyramidal (tetragonal) structure over tetrahedral coordination. If the coordination mode of the peroxide were a *trans*-μ-1,2 or a *cis*-μ-1,2 for $[Cu[HB(3,5\text{-}iPr_2pz)_3]]_2(O_2)$, a tetrahedral coordination geometry would be required which is not preferable for cupric ion. (A tetragonal type geometry with N_3O ligand arrangement is also disfavored with the hindered tripodal facial capping ligands.)

All three μ-η^2:η^2-peroxo complexes with tris(pyrazolyl)borate ligands exhibit essentially identical magnetic and spectral properties as summarized in Table 2. For instance, the diamagnetic property of $[Cu[HB(3,5\text{-}iPr_2pz)_3]]_2(O_2)$ is evident from its ^1H NMR spectrum consisting of very sharp signals located in the range of those observed for copper(I) complexes; no detectable contact shifts are seen. The diamagnetism is also supported by the magnetic susceptibility measurement in solution determined by the Evans method. Two characteristic intense absorption bands are observed at 349 (21 000) and 551 (790), both of which are assignable to $O_2^{2-} \rightarrow Cu(II)$ LMCT band, since no such bands are observed for other copper(II) complexes with the tris(pyrazolyl)borate ligand (more precise assignment is discussed below). The Raman spectrum of $[Cu[HB(3,5\text{-}iPr_2pz)_3]]_2(O_2)$ with 514.5-nm excitation gives the ν(O–O) band at 741 cm^{-1}, which is shifted to 698 cm^{-1} when the complex is prepared from $^{18}O_2$. No band attributable to ν(Cu–O) band is detected in the range of 400–600 cm^{-1}. Moreover, the Raman experiment with a 1:2:1 mixture of $^{16}O_2/^{16}O^{18}O/^{18}O_2$ clearly established the symmetric coordination mode of the peroxide in solution.

There was a possibility that the μ-η^2:η^2 structure was altered in solution, causing deformation to another coordination mode of the peroxide such as *trans*-1,2. In order to test this possibility, the spectroscopic comparison of the solid sample of the complex with the solution has been undertaken extensively. The much greater thermal stability of $[Cu[HB(3,5\text{-}Ph_2pz)_3]]_2(O_2)$ than $[Cu[HB(3,5\text{-}Me_2pz)_3]]_2(O_2)$ and $[Cu[HB(3,5\text{-}iPr_2pz)_3]]_2(O_2)$ in the solid state allowed the magnetic susceptibility measurement by the Faraday method at room temperature, which supported the diamagnetism.[33b] From variable-temperature magnetic susceptibilities of $[Cu[HB(3,5\text{-}iPr_2pz)_3]]_2(O_2)$, the $-2J$ was concluded to be more than 800 cm^{-1}.[37] The reflectance spectrum of the solid sample of $[Cu[HB(3,5\text{-}Ph_2pz)_3]]_2$-

Table 2. Properties of μ-Peroxo Dinuclear Cu(II) Complexes

compound	UV–vis (nm)	ν(O–O) (cm^{-1})	Cu–Cu (Å)	magnetism	ref(s)
$\{[Cu(Cyb)]_2(O_2)\}^{2+}$	550–600 (540)				52
$[Cu_2(XYL\text{-}O^-)(O_2)]^+$	385 (2900), 505 (6000), 610 (sh)	803	3.3[a]		40–42
$[Cu_2(N3PY2)(O_2)]^{2+}$	365 (15 000), 490 (5250), 600 (1200), >850 (—)		3.2[a]	EPR inactive	55
$[Cu_2(N4PY2)(O_2)]^{2+}$	360 (15 000), 458 (5000), 550 (1200), 775 (200)		3.4[a]	diamagnetic	55
$[Cu_2(N5PY2)(O_2)]^{2+}$	360 (21 400), 423 (3600), 520 (1200), >600 (—)			EPR inactive	55
$[Cu_2(N3OR)(O_2)]^{2+}$	350 (20 000), 485 (1400), 600 (880), 875 (sh)		3.3[a]	diamagnetic	55
$[Cu_2(XYL\text{-}F)(O_2)]^{2+}$	360 (18 700), 435 (4400), 515 (1300), 787(700), 925 (600)				57
$[Cu_2(UN)(O_2)]^{2+}$	360 (11 000), 520 (1000), 600 (sh)				59
$\{[Cu(TMPA)]_2(O_2)\}^{2+}$	440 (2000), 525 (11 500), 590 (7600), 1035 (160)	834	4.35	diamagnetic	29
$\{[Cu(BPIA)]_2(O_2)\}^{2+}$	440 (2000), 535 (11 500), 600 (7600)			EPR inactive	68
$\{[Cu(BPQA)]_2(O_2)\}^{2+}$	440 (2000), 535 (10 500), 600 (7600)				67
$\{[Cu(1,2\text{-}Me_2im)]_2(O_2)\}^{2+}$	346 (2200), 450 (1450), 500 (1900), 650 (600)		2.8 or 4.3[a]	EPR inactive	65,66
$[Cu_2(tpmc)(O_2)]^{2+}$	472 (2900), 780 (900)	820 and 771		EPR active	70
$[Cu_2(PY)_4N_6O(O_2)]^+$	390 (4800), 500 (6500), 630 (3400)				45
$[Cu_2(PY)_2(Pz)_2N_6O(O_2)]^+$	400 (2500), 505 (4900), 630 (3400)				45
$[Cu_2(PY)_2(DMP)_2N_6O(O_2)]^+$	390 (3400), 510 (6700), 630 (1600)				45
$\{Cu_2[Bz(NMI)_2N3]_2(O_2)\}^{2+}$	360 (—), 450 (—), 550 (—)				63
$\{Cu_2(FD)_2(DIEN)_2(O_2)\}^{2+}$	360 (—), 504 (1060)				61
$\{[Cu(CH_3PY2)_2(O_2)\}^{2+}$	355 (14 700), 405 (2500), 530 (400), 645 (315)				62
$\{[Cu(PhCH_2PY2)]_2(O_2)\}^{2+}$	362 (11 400), 415 (2600), 533 (650), 625 (480)				62
$\{[Cu(PhPY2)]_2(O_2)\}^{2+}$	350 (5500), 485 (310), 680 (70)				62
$[Cu_2(UN\text{-}O^-)(O_2)]^+$	392 (3400), 510 (5400), 642 (2700)		3.28[a]		46
$\{[Cu(N4\text{-}MePY)]_2(O_2)\}^{2+}$	440 (sh), 537 (5000), 610 (sh)				69
$\{[Cu(N4\text{-}Me_2PY)]_2(O_2)\}^{2+}$	378 (22 000), 494 (330), 784 (60)			diamagnetic	69
$[Cu(HB(3,5\text{-}Me_2pz)_3)]_2(O_2)$	338 (20 800), 530 (840)	731		diamagnetic	32
$[Cu(HB(3,5\text{-}iPr_2Pz)_3)]_2(O_2)$	349 (21 000), 551 (790)	741	3.56	diamagnetic	33
$[Cu(HB(3,5\text{-}Ph_2pz)_3)]_2(O_2)$	355 (18 000), 542 (1040)	759		diamagnetic	33
oxyhemocyanin	340 (20 000), 580 (100)	744–752	3.5–3.7[a]	diamagnetic	7–14
oxytyrosinase	345 (18 000), 600 (1200)	755	ca. 3.6[a]	diamagnetic	7–14

[a] Estimated by EXAFS.

(O_2) and mull absorption spectra of $[Cu[HB(3,5\text{-}iPr_2\text{-}pz)_3]]_2(O_2)$ exhibit two intense bands at ca. 350 and 550 nm whose features are identical to those of the solution spectrum.[37] The Raman spectra of solid samples of $[Cu[HB(3,5\text{-}Ph_2pz)_3]]_2(O_2)$ and $[Cu[HB(3,5\text{-}iPr_2pz)_3]]_2(O_2)$ exhibit the ν(O–O) band at 763 and 749 nm, respectively, which are nearly the same energies as the O–O stretch for the solutions.[33,37] Thus, the spectral features of solids are essentially the same as those observed for the solutions, indicating that the μ-η^2:η^2 structure is preserved in solution and that the unique properties are intrinsic to the μ-η^2:η^2 structure.

The resonance enhancement profile for the ν(O–O) Raman feature has been explored for $[Cu[HB(3,5\text{-}iPr_2\text{-}pz)_3]]_2(O_2)$, indicating that excitation of both 350 and 550-nm bands enhance the ν(O–O) band.[37] Hence, these two characteristic bands are assigned to peroxide-to-copper charge-transfer transitions. As described in the review by Solomon et al. in this issue, the π^* orbital of a side-on bound peroxide including the μ-η^2:η^2-peroxide splits into two energies designated as π^*_v and π^*_σ, depending upon the orientation to the $d_{x^2-y^2}$ orbital in which the unpaired electron of the cupric ion lies. Because the intensity of the peroxide-to-copper LMCT band reflects the overlapping population between the π^* orbital of peroxide and the d orbital of cupric ion, the intensity of the $\pi^*_v \rightarrow$ Cu(II) transition is in general lower than that of $\pi^*_\sigma \rightarrow$ Cu(II). Accordingly, the 350- and 550-nm bands are assignable to the $\pi^*_\sigma \rightarrow$ Cu(II) and $\pi^*_v \rightarrow$ Cu(II) LMCT transition, respectively. The Raman and IR spectra of a solid sample of $[Cu[HB(3,5\text{-}Ph_2pz)_3]]_2(O_2)$ have been examined in detail.[37] A broad band is observed in the Raman spectrum at 1144 cm^{-1} which is shifted to 1098 cm^{-1} upon isotopic substitution. This band is attributable to the overtone of the ν(Cu–O) band whose fundamental vibration frequency is 572 cm^{-1}. The fundamental vibration is, however, not observed because it is a symmetrically forbidden transition. Another isotopically susceptible band is detected at 331 cm^{-1} in the IR spectrum, which was assigned to the B_{2u} vibration mode of the Cu_2O_2 chromophore.[37] On the basis of these vibrational data, the O–O force constant, which is correlated with the O–O bond strength directly, was determined by normal coordinate analysis, for the μ-η^2:η^2-peroxide to be 2.4 mdyn/Å. Since the O–O force constants calculated for a *trans*-μ-1,2-peroxo complex and an asymmetric terminal peroxo complex (vide infra) are 3.1 and 2.9 mdyn/Å, respectively, the O–O bond strength in the μ-η^2:η^2-peroxo complex is weakened significantly as compared with other structural types of peroxo complexes.

In order to provide a theoretical basis for understanding the unusual properties of the μ-η^2:η^2-peroxo complexes, extended Hückel[33b] and SCF-Xα-SW[38,39] calculations have been carried out. The theoretical treatment and the interpretation of the μ-η^2:η^2-peroxo complex based on SCF-Xα-SW calculations is described in detail in the review by Solomon in this issue. These calculations endorse the enormously strong antiferromagnetic property of the μ-η^2:η^2-peroxo complex resulting in seeming diamagnetism even at room temperature. The HOMO and LUMO orbitals derived from the Hückel calculations are schematically indicated in Figure 5.[33b] The strong antibonding nature between Cu d_{yz} and O_2 π^*_σ is evident in the LUMO, while the HOMO orbital interaction is nearly negligible. The strong destabilizing interaction in LUMO thus causes an enormously large HOMO–LUMO gap, accounting for the strong antiferromagnetic coupling between the two cupric ions through the μ-η^2:η^2-peroxide ion. Al-

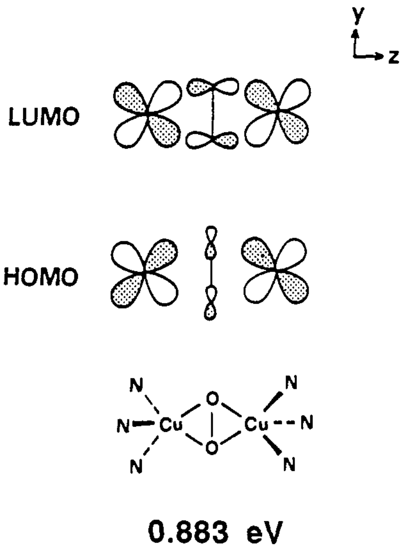

Figure 5. HOMO–LUMO orbitals of $[(NH_3)_3Cu]_2(O_2)$ calculated by extended Hückel calculations. (Reprinted from ref 33b. Copyright 1992 American Chemical Society.)

though the model used for the SCF-Xα-SW calculations is not the same as that used for Hückel calculations, the HOMO and LUMO have orbital shapes very similar to those shown in Figure 5. A large HOMO–LUMO gap is also noticed which gives rise to an $-2J$ value as great as 5660 cm^{-1}.[38] Another notable result derived from the SCF-Xα-SW calculations is a considerable interaction in the HOMO orbitals between the O_2^{2-} σ^* and Cu $d_{x^2-y^2}$. This indicates that O_2^{2-} σ^* acts as a π-acid, which accepts electron density from the cupric ions. Since the O_2^{2-} σ^* is an antibonding orbital, this interaction weakens the O–O bond significantly, accounting for the unusually low ν(O–O) and more directly the small O–O force constant of the μ-η^2:η^2-peroxo complex. The SCF-Xα-SW calculations further led to estimates of the energies of the transitions from O_2^{2-} π^*_v and π^*_σ to cupric ion, which lends support to the assignment of the 350- and 550-nm bands to O_2^{2-} π^*_σ → Cu(II) and O_2^{2-} π^*_v → Cu(II) LMCT transitions, respectively.[37]

C. Terminal-Peroxo Complexes

A dinuclear copper(I) complex with a dinucleating ligand XYL-O$^-$ having a phenoxo bridging group was demonstrated to bind dioxygen at low temperature quasi-reversibly, yielding an intensely purple colored complex.[40] The ν(O–O) of 803 cm^{-1} ascertained by resonance Raman spectroscopy as well as the dioxygen absorption stoichiometry (Cu/O_2 = 2) suggested that the formed dioxygen adduct is a peroxo complex. $[Cu_2(XYL\text{-}O^-)(O_2)]^+$ exhibits visible bands at 385 (2900), 505 (ca. 6000), and 787 (700), with a shoulder at 610 nm. The 385-nm band is assigned to phenoxo-to-copper LMCT band while the 787-nm band is attributable to the d–d transition of the cupric ion. A Gaussian resolution of the spectrum reveals the feature around 600 nm to be a strong band at 503 (6300) with a weaker component at 625 (1100).[41] Besides the ν(O–O) band, the detailed resonance Raman study on $[Cu_2(XYL\text{-}O^-)(O_2)]^+$ indicated an isotopically susceptible band at 488 cm^{-1} which was assigned to ν(Cu–O) band.[41] The intensity of ν(O–O) band showed significant enhancement from both the 503- and 625-nm absorption bands, indicating that these two absorption bands are attributable to peroxide-to-copper charge-transfer transitions. The ν(Cu–O) band is also enhanced with 503-nm excitation, but less enhanced from the 625-nm transition. In conjunction with the SCF-Xα-SW calculations, the bands at 503 and 625 nm are assigned to O_2^{2-} π^*_σ → Cu(II) and O_2^{2-} π^*_v → Cu(II) LMCT band, respectively. While from the ligand structure, a *cis*-μ-1,2 coordination mode of the peroxide was expected, the Raman experiments with mixed-labeled dioxygen excluded this possibility, rather the terminal type coordination mode of the peroxide was strongly suggested.[41] On the other hand, EXAFS results indicated that the Cu···Cu separation is 3.3 Å for $[Cu_2(XYL\text{-}O^-)(O_2)]^+$.[42] This rules out a μ-1,1 bridging structure since the crystal structures of other complexes with the phenoxo bridging ligand XYL-O$^-$ show that a μ-1,1 geometry is only compatible with a Cu···Cu separation of less than 3.15 Å.[43,44] Hence, the asymmetric terminal coordination mode of the peroxide with a weak interaction between the free end of the peroxide and the second copper was concluded to be the most plausible structure.

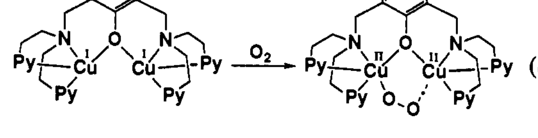

(eq 12)

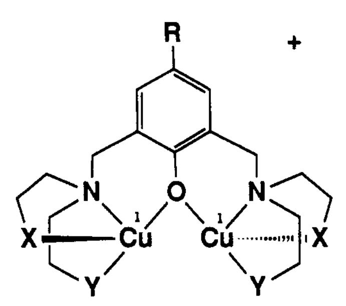

R = H, X = Y = 2-pyridyl (XYL-O$^-$)
R = Me, X = Y = 2-pyridyl ($(Py)_4N_6O$)
R = Me, X = Y = 1-pyrazolyl
R = Me, X = Y = 1-(3,5-dimethypyrazolyl)
R = Me, X = 2-pyridyl, Y = 1-pyrazolyl ($(Py)_2(Pz)_2N_6O$)
R = Me, X = 2-pyridyl, Y = 1-(3,5-dimethylpyrazolyl) ($(Py)_2(DMP)_2N_6O$)

Figure 6. Dinucleating ligands having a phenoxo bridge.

A series of copper(I) complexes with a dinucleating ligand containing the same xylyl frame as in XYL-O$^-$ in which, however, the side-arm pyridine donors are replaced with other N-ligand donors such as pyrazole were prepared (Figure 6).[45] Among these complexes, the copper(I) complexes having the ligands with all four pyridyl groups substituted with 1-pyrazolyl or 1-(3,5-dimethylpyrazolyl) were not stable due to disproportionation. However, the other complexes are reactive toward dioxygen affording the peroxo complexes at −78 °C in CH_2Cl_2. For instance, the complex with two pyridyl and two 3,5-dimethylpyrazolyl groups yielded a dioxygen adduct which exhibits the visible bands at 390 (3400) and 510 (6700) with a shoulder at 630 nm.[45] Other dioxygen adducts give rise to the similar visible spectra. Because these features are in excellent accord

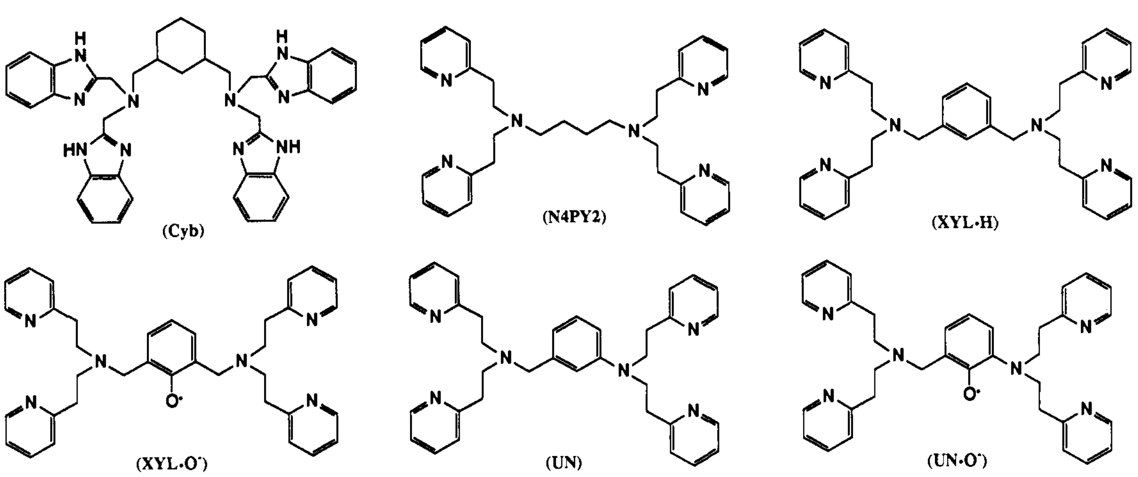

Figure 7. Dinucleating ligands effective for preparing μ-peroxo–copper complexes.

with that of $[Cu_2(XYL\text{-}O^-)(O_2)]^+$, the coordination mode of the peroxide is suggested to be asymmetric terminal. When these dioxygen complexes were allowed to warm to room temperature, irreversible decomposition occurred, resulting in formation of a μ-hydroxo dinuclear copper(II) complex.[45]

Very recently, an unsymmetric ligand having a phenoxo bridging group (designated as UN-O⁻ whose structure is shown in Figure 7) has been prepared.[46] The dinuclear copper(I) complex with this ligand reacts with dioxygen reversibly at −80 °C, giving an intensely purple solution with LMCT absorption maxima at 392 (3400), 510 (5400), and 642 (2700). The coordination mode of the peroxide in $[Cu_2(UN\text{-}O^-)(O_2)]^+$ is presumably the same as that in $[Cu_2(XYL\text{-}O^-)(O_2)]^+$ on the basis of its spectral similarity. This complex is much superior in terms of thermal stability and thus its isolation in a solid state form was successfully achieved.[46]

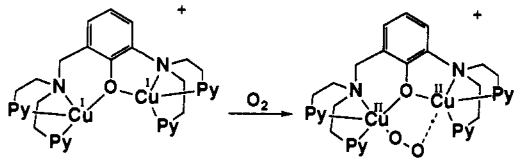

(eq 13)

D. Other Complexes

As described above, there are two alternative reaction pathways to prepare the μ-peroxo dinuclear complexes starting from copper(I) complexes. One preparation method is dioxygen addition to a dinuclear copper(I) complex having a dinucleating ligand. The other one is the self-assembly of a monomeric copper(I) precursor in the presence of dioxygen. In both cases, the copper(I) center must be coordinatively unsaturated and thus the maximum number of the ligand donors employed is four. The first demonstration of the beneficial use of a dinucleating ligand in preparing a μ-peroxo complex was demonstrated by Osborn et al.,[47] whereas the self-assembly was first reported by Wilson et al.[48] Both contributions were accomplished in late 1970s. Unfortunately, the characterization of the dioxygen adduct was not credible,[49] since no solid evidence supporting the μ-peroxo structure was provided. Particularly, the self-assembly formation of the μ-peroxo complex was carried out with a N_5 ligand, which does not satisfy the above criterion, and thus the formation of the μ-peroxo complex may be debatable.[50,51] In conjunction with low-temperature spectroscopy, much more extensive endeavors to synthesize and characterize μ-peroxo dinuclear copper(II) complexes including the examples described already have been undertaken recently; these attempts were also carried out on the basis of the same synthetic strategies applied for these earlier works.

1. N_3–N_3 Dinucleating Ligand System

A dinuclear copper(I) complex formed in situ between $Cu(MeCN)_4BF_4$ and a dinucleating ligand containing a cyclohexyl spacer with four arms consisting of 2-benzylimidazole (Cyb in Figure 7) reacts with air at 5 °C, causing a color change of the solution from pale yellow to deep violet.[52] A broad intense band was observed at 550–600 nm with a minimum absorption coefficient estimated to be 540 $cm^{-1}\,M^{-1}/2Cu$. The violet solution showed no apparent change at 0 °C for 30 min. When nitrogen was bubbled through the solution, the violet color disappeared gradually and bubbling of dioxygen again gave the violet solution. Thus, the copper(I) complex binds dioxygen reversibly. Unfortunately, the structure of the formed dioxygen adduct has not been identified fully.

Karlin and co-workers reported the synthesis of a dinuclear copper(I) complex with a ligand in which two bis(2-pyridylethyl)amine units are linked with an *n*-butyl chain (N4PY2 in Figure 7).[53] This dinuclear copper(I) complex reacts with dioxygen at low temperature quasi-reversibly. The dioxygen adduct shows visible bands at 360 (15 000), 458 (5000), and 550 (1200) with a d–d band at 775 (200). Although resonance Raman spectroscopy was not applied because of its instability under photoirradiation, from the dioxygen consumption amount, the dioxygen adduct was suggested to be a μ-peroxo dinuclear complex formulated as $[Cu_2(N4PY2)(O_2)]^{2+}$. The dinuclear structure of the oxygenated species was also supported from the observation that the complex is EPR silent, which is attributable to the strong antiferromagnetic coupling between the two cupric ions through the peroxide ion. The recent evaluation[30] showed that the complex is virtually diamagnetic. On the basis of EXAFS studies which estimated the Cu···Cu separation of ca. 3.4 Å, a *cis*-μ-peroxo or a bent μ-η^2:η^2 structure was suggested.[54] However, an X-ray crystal structure of this complex has not been successfully determined yet.

Similar dinucleating ligands with variation of the methylene spacer to *n*-propyl and *n*-pentyl chains have been prepared.[53,55] Both dioxygen adducts obtained with these ligands exhibit three characteristic bands at ca. 360, 400–500, and 500–600 nm, similar to those of $[Cu(N4PY2)(O_2)]^{2+}$. The resemblance implies the formation of a μ-peroxo complex in which the coordination mode of the peroxide is essentially identical to that of $[Cu_2(N4PY2)(O_2)]^{2+}$. However, as summarized in Table 2, there are significant differences seen in the absorption wave numbers, absorption coefficients, and Cu···Cu separations (estimated for the complex with N3PY2 to be 3.2 Å by EXAFS). These differences may reflect structural variations in the Cu_2O_2 chromophore possibly associated with ligand constrains due to the spacer size.

A related dinuclear copper(I) complex was prepared with a ligand having an arene spacer referred to as XYL-H in Figure 7.[43,56] When this complex was treated with dioxygen, instantaneous hydroxylation yielding a phenoxo-bridged dinuclear copper(II) complex occurred. This type of ligand hydroxylation will be described later in this review. Although an intermediate was observed transiently in the hydroxylation reaction, it was too unstable to be characterized. However, when the 1-position of the arene ring was substituted with floride to inhibit the hydroxylation, a relatively stable dioxygen adduct was trapped.[57] This complex exhibits characteristic absorption bands at 360 (18 700), 435 (4400), and 515 (1300). Since the spectral features are reasonably in accord with that of $[Cu_2(N4PY2)(O_2)]^{2+}$, the coordination mode of the peroxide was suggested to be identical. Formation of a similar dioxygen adduct was noted when a chloro-substituted ligand (XYL-Cl) was employed.[58] An unsymmetrical dinucleating ligand UN with an arene bridge was prepared (see Figure 7).[59] It is of interest that the stability of the dioxygen adduct is much enhanced with this ligand as compared with the one prepared with XYL-H. Accordingly, the dinuclear copper(I) complex reacts with dioxygen at −80 °C, forming a μ-peroxo complex (on the basis of dioxygen consumption) which exhibits visible bands at 360 (11 000) and 520 (1000) with a shoulder band at 600 nm. From its resemblance, the structure of the dioxygen adduct was demonstrated to be similar to that of $[Cu_2(N4PY2)(O_2)]^{2+}$. However, it is noteworthy that the spectrum is more similar to the μ-η^2:η^2-peroxo complex $[Cu(HB(3,5\text{-}iPr_2pz)_3)]_2(O_2)$, since there is no intense band in 400–500-nm region. Whereas the reaction of $[Cu_2(XYL\text{-}H)]^{2+}$ with dioxygen is rapid and irreversible even at −80 °C, dioxygen binding to $[Cu_2(UN)]^{2+}$ is reversible. Thus, when the solution of the latter dioxygen adduct generated at −80 °C was heated briefly and evacuated under a vacuum, decoloration and reversion of the reduced dinuclear copper(I) complex were effected. Four oxygenation/deoxygenation cycles can be carried out without severe decomposition (~20%). When the dinuclear copper(I) complex was treated with dioxygen above 0 °C, hydroxylation of 1-position of the arene ring as observed for $[Cu_2(XYL\text{-}H)]^{2+}$ occurred.[59]

A macrocyclic ligand having N_6 ligand donors $MX_2(DIEN)_2$ was used for preparing a dinuclear copper(I) complex. An aerobic reaction of the ligand with 2 equiv of $Cu^I(MeCN)_4(ClO_4)$ gave $[Cu_2(MX_2(DIEN)_2)]^{2+}$. When the complex was exposed to dioxygen at room temperature, hydroxylation of the one arene ring proceeded (see eq 17) and no stable dioxygen adduct was obtained.[60] To inhibit the aromatic hydroxylation, the phenyl ring was replaced with furan. The dinuclear copper(I) complex with the ligand $(FD)_2(DIEN)_2$ absorbs ca. 0.5 equiv of dioxygen at 5 °C, suggesting the formation of a μ-peroxo dinuclear copper(II) complex.[61] The complex is not very stable and the reaction is followed by slower dioxygen uptake due to irreversible degradation to give a dinuclear copper(II) complex. (In the presence of methanol, the product was identified as $[Cu_2[(FD)_2(DIEN)_2](OH)(OMe)]^{2+}$.) The transiently formed μ-peroxo complex exhibits two intense absorption bands at 360 and 504 (1060), which are attributable to peroxide-to-copper charge-transfer transitions.

2. Self-Assembly of Monomer with N_3 Ligand

Since the dinucleating ligands containing bis(2-pyridylethyl)amine moieties are effective for preparing a μ-peroxo dinuclear copper(II) complex as described already, monomeric copper(I) complexes derived with the tridentate ligands R-substituted bis(2-pyridylethyl)amines (see Figure 8) were explored to test whether they could afford μ-peroxo complexes. The structure of $[Cu(PhPY2)]^+$ was determined by X-ray crystallography, establishing a nearly T-shape structure.[62] The complexes $[Cu(RPY2)]^+$ react with dioxygen in a stoichiometry of Cu/O_2 = 4:1 above 0 °C, implying the formation of μ-oxo dinuclear copper(II) complexes. However, at −80 °C, the stoichiometry is 2:1 for Cu/O_2, and the resulting copper(II) complexes exhibit characteristic absorption bands.[62] For instance, $\{[Cu(CH_3PY2)]_2(O_2)\}^{2+}$ gives absorption bands at 355 (14 700), 405 (2500), 530 (400), and 645 (315). The other complexes show similar spectra. Although the intensity of the band at ca. 400 nm is considerably lower, the overall features of the spectra are almost in accord with that of $[Cu_2(N4PY2)(O_2)]^{2+}$, implying that the complexes derived from the monomeric precursors adopt a μ-peroxo coordination mode close to that of $[Cu_2(N4PY2)(O_2)]^{2+}$.

A series of similar tridentate ligands containing imidazole groups instead of pyridine has been synthesized.[63] Among these complexes, only the copper(I) complexes with $Bz(NMI)_2N3$ and $Bz(NBzI)_2N3$ react with dioxygen at −80 °C. On the basis of the visible spectral features, the oxygenated species has been identified as a μ-peroxo dinuclear copper(II) complex whose structure is similar to that of $[Cu(CH_3PY2)]_2(O_2)$.

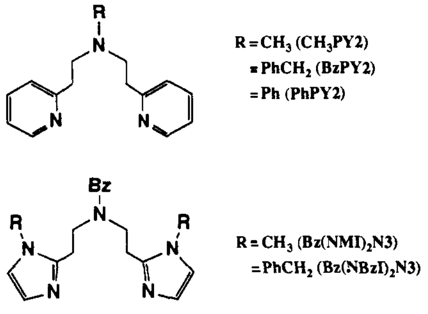

Figure 8. Tridentate chelating ligands explored to generate μ-peroxo–copper complexes.

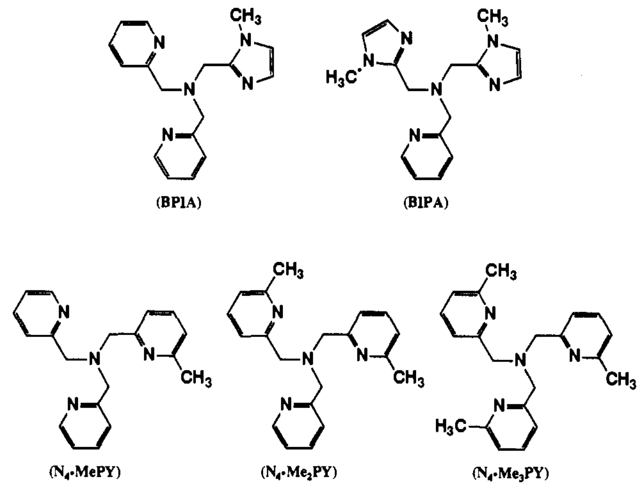

Figure 9. N_4 ligands analogous to TMPA.

Very recently, a tridentate N_3 ligand in which one of 6-methyl-2-pyridyl groups in a tetradentate N_4 ligand N_4-Me_3PY (see Figure 9) was replaced with phenyl was prepared.[64] The ligand is essentially analogous to $PhCH_2PY2$, although the chelating size is different. The copper(I) complex with the ligand binds dioxygen at −70 °C. The oxygenated complex exhibits no band at 400–500 nm, but gives rise to two characteristic bands at 360 and 540 nm. The spectral feature is very similar to that of $[Cu[HB(3,5\text{-}iPr_2pz)_3]]_2(O_2)$, indicative of the formation of a μ-η^2:η^2-peroxo complex.

To provide insights into the structural factors which control dioxygen binding and activation in imidazole (histidine) ligated copper proteins, monomeric copper(I) complexes with 1,2-dimethylimidazole (1,2-Me_2im) have been prepared and their reactivity toward dioxygen was examined.[65] Anaerobic treatment of $[Cu(CH_3CN)_4](PF_6)$ with 2 equiv of 1,2-Me_2im gave a linear two-coordinate complex which does not react with dioxygen.[66] However, one additional molar equivalent of 1,2-Me_2im yielded a putative three-coordinate complex which reacted with dioxygen readily, producing a dioxygen adduct. The dioxygen adduct is EPR silent and exhibits four characteristic absorption bands: 346 (2200), 450 (1450), 500 (1900), and 650 (600).[65] Although the EXAFS of the dioxygen adduct is more consistent with a bent μ-η^2:η^2-peroxo bridging structure with 2.84-Å Cu···Cu separation, the UV–vis spectroscopic properties and the reactivity (described later) suggested a *trans*-μ-1,2-peroxo structure as a more likely model.[66]

3. N_4 Ligand System

As described already, a monomeric copper(I) complex with a tripodal tetradentate ligand TMPA or a 2-quinolyl-substituted derivative BPQA reacts with dioxygen at low temperature to give a relatively stable *trans*-μ-1,2-peroxo complex.[27b,67] As related ligand systems, imidazolyl-containing ligands BPIA and BIPA (Figure 9) have been synthesized, and the reaction of the copper(I) complexes with these ligands and dioxygen was explored.[68] The X-ray analysis of $[(BPIA)_2Cu_2]^{2+}$ revealed a dimeric structure, in which each copper(I) ion is coordinated in a trigonal pyramidal N_4 environment with ligation of the imidazolyl group of the BPIA donor to the adjacent copper(I) ion. Conductivity measurements indicated that the copper(I) complexes are monomeric in EtCN, and thus formed $[(BPIA)Cu(EtCN)]^+$ and $[(BIPA)Cu(EtCN)]^+$. Low-temperature oxygenation of $[(BPIA)Cu(EtCN)]^+$ resulted in the generation of a *trans*-μ-1,2-peroxo complex which was confirmed on the basis of manometric measurements, its EPR silence, and close similarity of its UV–vis spectrum compared to that of $\{[(TMPA)Cu]_2(O_2)\}^{2+}$. By contrast, $[(BIPA)Cu(EtCN)]^+$ reacted with dioxygen at −80 °C to give an intensely red-colored solution (λ_{max} = 330 nm), but the dioxygen adduct is unstable and not characterized fully.[68]

Suzuki et al. synthesized a series of tetradentate ligands N_4-Me_nPY (n = 1–3) in which 6-methyl groups are introduced into TMPA (Figure 9).[69] The oxygenated product formed from a copper(I) precursor with N_4-MePY showed a visible spectrum identical to that of $\{[Cu(TMPA)]_2(O_2)\}^{2+}$, indicated formation of a *trans*-μ-1,2-peroxo complex. Whereas the monomeric copper(I) complex with N_4-Me_3PY was inert toward dioxygen at low temperature, N_4-Me_2PY reacted with dioxygen at −70 °C reversibly. The electronic spectrum of the oxygenated complex showed an intense band at 378 (22 000) with two weak bands at 494 (330) and 784 (60). The dioxygen uptake was ca. 0.5 per mole of the monomeric copper(I) precursor, suggesting formation of a μ-peroxo complex, yet the spectrum is clearly distinctive from $\{[Cu(TMPA)]_2(O_2)\}^{2+}$. The structural identification of the oxygenated species remains to be determined.[69]

A dinuclear copper(I) complex with a macrocyclic N_8 ligand tmpc was prepared and its reactivity toward dioxygen was explored.[70] The dinuclear structure of the copper(I) complex was established by X-ray crystallography. The coordination geometry about each copper atom is best described as a distorted trigonal. The basal plane consists of one nitrogen from the ligand frame amine and two pyridyl nitrogens from pendant groups. The remaining amine nitrogen is not coordinated to the copper. When the copper(I) complex was treated with dioxygen at −85 °C, the electronic spectrum exhibited two bands at 472 (2900) and 700 (900). The excitation of the 472-nm band enhances Raman bands at 820 and 771 cm^{-1}, which are shifted to 773 and 727 cm^{-1}, respectively, upon isotopic substitution with $^{18}O_2$. This result is indicative of the formation of two structurally distinct μ-peroxo complexes, which were proposed to be intra and inter peroxo-bridged complexes.[70] From the structures of other dinuclear copper(II) complexes with tpmc $[Cu_2X(tpmc)]^{3+}$ (X = F^-, Cl^-, Br^-, OH^-, N_3^-, NO_2^-, or $MeCOO^-$), each copper(II) ion in the intraligand μ-peroxo complex was proposed to possess a five-coordinate structure with a N_4O ligand donor set, while the coordination mode of the peroxide is still ambiguous.

E. Spectral Criteria for Structural Classification

As summarized in Table 2, μ-peroxo dinuclear copper(II) complexes exhibit characteristic spectral features depending upon the coordination mode of the peroxide. While the spectroscopic characterization has not been completely pursued due to thermal instability, UV–vis spectral data are available for all complexes. The μ-η^2:η^2-peroxo complex, whose structure has been definitely established by X-ray crystallography, gives intense bands at ~350 (20 000) and ~550 (1000). On the other hand, the other structurally determined *trans*-μ-1,2 peroxo complex gives characteristic bands at 440 (2000) and 525 (11 500) with a shoulder at ca. 600 nm. On the basis of the similarities of the spectral features and ligand donors, some of the complexes reported to date are reasonably suggested to possess either of these coordination modes of peroxide. A number of complexes with N_3–N_3 dinucleating ligands exhibit three characteristic bands at ca. 360 (15 000–20 000), 420–490 (1500–5500), and 520–600 (1000). From the ligand structures and the Cu···Cu separation estimated by EXAFS, *cis*-μ-1,2 and bent μ-η^2:η^2 structures have been proposed, with the latter structure demonstrated to be more plausible. Given the structure as a bent μ-η^2:η^2, the ca. 350- and 520–600-nm bands are ascribed to $\pi^*_\sigma \rightarrow$ Cu(II) and $\pi^*_v \rightarrow$ Cu(II) LMCT bands, respectively, by analogy to [Cu[HB(3,5-iPr$_2$pz)$_3$]]$_2$(O$_2$). The other 420–490-nm band may be ascribed to another $O_2^{2-} \rightarrow$ Cu(II) LMCT transition which is forbidden for the symmetric planar μ-η^2:η^2-peroxide but allowed when the Cu_2O_2 chromophore is bent. The variations in the wavelength maxima and absorption coefficients particularly of the 420–490-nm band may reflect the degree of bending depending on the ligand spacer size. While these interpretations seem to be reasonable, more credible structural identifications, ultimately X-ray structures of the supposed bent μ-η^2:η^2-peroxo complex will be required. The well-characterized phenoxo-bridged peroxo complexes adopting an unsymmetrical terminal coordination mode gives two characteristic bands at 505 (6000) with a shoulder at ca. 620 nm. No intense band is observed for this structural type complex in the region of 300–500 nm except the band at ca. 400 (3000–4000), which is assignable to a phenoxo-to-copper charge-transfer band. Hence, the UV–vis spectral features appear to be a good index to distinguish the coordination mode of peroxide. However, it is noteworthy that these criteria are only applicable to complexes having comparable ligand systems, because the peroxide-to-copper charge-transfer transition is strongly dependent on the orientation of the copper d lobe of an unpaired electron with respect to the peroxide π^* orbital. Thus the complex with a N_4–N_4 ligand, for instance, gives rise to distinctive spectral features from that of N_3–N_3 ligand complexes.[70]

F. Reactivity of the Peroxo Complexes

1. μ-η^2:η^2-Peroxo Complexes

The reactivity of the planar μ-η^2:η^2-peroxo complex [Cu[HB(3,5-Me$_2$pz)$_3$]]$_2$(O$_2$) has been explored.[71] This complex is not thermally very stable and, thus, spontaneously decomposes to a putative μ-oxo dinuclear copper(II) complex [Cu[HB(3,5-Me$_2$pz)$_3$]]$_2$O with evolution of dioxygen at room temperature. This spontaneous decomposition is interpreted in terms of a mechanism involving O–O bond homolysis of the peroxide as illustrated in Figure 10. The Cu(II)–O$^\bullet$ radical generated in the O–O bond homolysis as proposed for μ-peroxo dinuclear iron(III) complexes[72] couples with a copper(I) complex which is in equilibrium with the peroxo complex at room temperature in a solution, yielding the μ-oxo complex. Support for the existence of an equilibrium between the μ-η^2:η^2-peroxo complex and a copper(I) species lies on the observation that the addition of PPh$_3$ or CO to a solution of the μ-η^2:η^2-peroxo complex at room temperature results in instantaneous reductive ligand displacement to afford the corresponding copper(I) complexes, Cu(PPh$_3$)[HB(3,5-Me$_2$pz)$_3$] and Cu(CO)[HB(3,5-Me$_2$pz)$_3$], respectively, with evolution of dioxygen. The first-order dependence of the consumption rate of [Cu[HB(3,5-Me$_2$pz)$_3$]]$_2$(O$_2$) with respect to its concentration in the spontaneous decomposition is also in accord with the mechanism, if the O–O bond homolysis is the rate-determining step.[71]

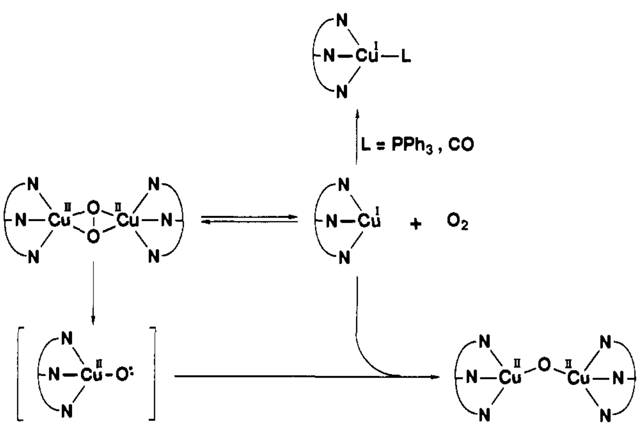

Figure 10. Homolytic cleavage proposed for μ-η^2:η^2-peroxo-dicopper(II) complex.

The Cu(II)–O$^\bullet$ species formed in the O–O bond homolysis functions as a weak hydrogen acceptor so as to react with cyclohexene to generate a cyclohexyl radical. Accordingly, under argon in CH$_2$Cl$_2$, the spontaneous decomposition of [Cu[HB(3,5-Me$_2$pz)$_3$]]$_2$(O$_2$) in the presence of cyclohexene results in formation of 1-chloro-2-cyclohexane in a low yield, whereas under dioxygen, 2-cyclohexen-1-one and 2-cyclohexen-1-ol are formed catalytically. Only a trace amount of cycloxene oxide is obtained. The labeling experiment indicated that the incorporated oxygen atom in the products comes from the exogenous dioxygen but not from the μ-η^2:η^2-peroxide. Moreover, the rate of consumption of [Cu[HB(3,5-Me$_2$pz)$_3$]]$_2$(O$_2$) in the presence of cyclohexene/dioxygen is identical to the spontaneous decomposition rate under argon. Therefore, the catalytic oxidation of cyclohexene under a dioxygen atmosphere was suggested to proceed by the classical radical chain reactions initiated by hydrogen atom abstraction from cyclohexene with the Cu(II)–O$^\bullet$ intermediate. The oxidizing capability of the Cu(II)–O$^\bullet$ generated from [Cu[HB(3,5-Me$_2$pz)$_3$]]$_2$(O$_2$) is not markedly high and the complex is ineffective for oxidations of other substrates including sulfides and alkanes.

As described below, the μ-η^2:η^2-peroxo serves as a synthetic model for not only oxyhemocyanin but also oxytyrosinase, whose properties are extremely similar to those of oxyhemocyanin, Since tyrosinase catalyzes the oxidation of phenols, particularly tyrosine, the reaction of [Cu[HB(3,5-Me$_2$pz)$_3$]]$_2$(O$_2$) with phenols was examined. The anaerobic reactions gave diphenoquinones as sole products, whereas under aerobic conditions, the oxidations proceed much faster and benzoquinones are also formed as minor products.[71] The formation of diphenoquinones as major products strongly suggests a free-radical-type reaction mechanism via a phenoxo radical as a reaction intermediate. In fact, kinetic experiments indicated that there are two distinct reaction pathways responsible for the formation of a phenoxo radical.[71] One reaction step is the H$^\bullet$ radical abstraction from a phenol by the Cu(II)–O$^\bullet$ radical generated by the O–O bond homolysis. The other reaction pathway is the acid/base reaction of $[Cu[HB(3,5\text{-}Me_2pz)_3]]_2(O_2)$ with a phenol resulting in formation of a phenoxo cupric complex initially, followed by Cu–O homolysis to afford a phenoxo radical. This reaction is competitive to the H$^\bullet$ abstraction pathway of a phenol, being faster when the concentration of the phenol is high and/or at low temperature where the rate of the O–O bond homolysis is negligible. The diphenoquinones are yielded by the oxidative coupling of the phenoxo radical, the mechanism of which is well established as a classical type radical reaction. The formation of benzoquinones, on the other hand, was ascribed to the direct addition of dioxygen to the phenoxo intermediate to form a peroxy phenoxo radical. The reaction is accelerated due to the resonance structure of the cupric phenoxo complex as indicated in eq 14. The ortho (or para) position of a phenoxide coordinated to cupric ion is more accessible to a radical addition due to the contribution of its radical structure than that of the free phenol. Although the phenoxo complex could not be isolated in the reaction system with $[Cu[HB(3,5\text{-}Me_2pz)_3]]_2(O_2)$, the low-temperature reaction of $[Cu[HB(3,5\text{-}iPr_2pz)_3]]_2(O_2)$ and a phenol such as *p*-fluorophenol gave a phenoxo–copper(II) complex which is isolable; $Cu(OC_6H_4\text{-}p\text{-}F)[HB(3,5\text{-}iPr_2pz)_3]$ was structurally characterized by X-ray crystallography.[73] This result is indicative of the nucleophilic property of the $\mu\text{-}\eta^2{:}\eta^2$-peroxo complexes.

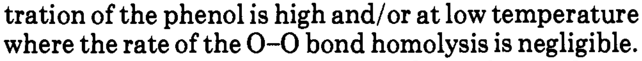

(eq 14)

The reactivity of $[Cu_2(N4PY2)(O_2)]^{2+}$ has been explored in detail.[74] The X-ray structure of the complex is not available; however, as described above, a bent $\mu\text{-}\eta^2{:}\eta^2$ structure is suggested to be the most plausible. The reaction of the complex with CO causes the stoichiometric displacement of the bound dioxygen, affording the CO adduct as does $[Cu[HB(3,5\text{-}Me_2pz)_3]]_2(O_2)$. However, $[Cu(N4PY2)(O_2)]^{2+}$ oxidizes PPh_3 to $OPPh_3$ quantitatively. Whereas the other structural complexes $[Cu_2(XYL\text{-}O^-)(O_2)]^+$ and $\{[Cu(TMPA)]_2(O_2)\}^{2+}$ are reactive, $[Cu_2(N4PY2)(O_2)]^{2+}$ is inert toward protonation and acylation, indicative of its relatively low nucleophilic reactivity. This behavior is also consistent with the observation that $[Cu_2(N4PY2)(O_2)]^{2+}$ does not react with an electrophile CO_2, while it reacts with SO_2 to give $[Cu_2(N4PY2)(SO_4)(MeCN)_2]^{2+}$. The fact that $[Cu_2(N4PY2)(O_2)]^{2+}$ is less nucleophilic than planar $\mu\text{-}\eta^2{:}\eta^2$-peroxo complexes may be associated with the bent structure. The reaction pattern toward phenol is, however, very similar; 2,4-di-*tert*-butylphenol is oxidized to 3,3′,5,5′-tetra-*tert*-butyl-2,2′-dihydroxybiphenol, an apparent radical coupling product.[74]

Anaerobic reactions of $\{Cu_2[(FD)_2(DIEN)_2](O_2)\}^{2+}$ with phenols and related compounds give the corresponding radical coupling product selectively, as seen for the reaction between $[Cu[HB(3,5\text{-}Me_2pz)_2]](O_2)$ and phenols.[75] A copper(II) complex obtained from $CuCl_2$ and $(FD)_2(DIEN)_2$ in methanol, presumably a methoxo complex, is also effective for oxidation of phenols but its activity is much lower, and virtually ineffective for oxidations of 3,5-di-*tert*-butylcatechol and 3,4-dimethylaniline. Since both of the substrates are not oxidized catalytically under dioxygen, whereas the other phenols are oxidized, it seems likely that the copper(II)-catalyzed oxidation is a necessary part of the catalytic activity in the presence of excess dioxygen. Although the mechanism of the reaction between the peroxo complex and phenols remains to be elucidated, the oxidation of phenol presumably proceeds via a phenoxo–copper(II) intermediate as proposed for the oxidation of phenols with $[Cu[HB(3,5\text{-}Me_2pz)_3]]_2(O_2)$.[71]

2. Other Structural Complexes

The reactivity patterns of two structurally distinct peroxo complexes were compared with that of $[Cu_2(N4PY2)(O_2)]^{2+}$.[74] Both terminal peroxo complex $[Cu_2(XYL\text{-}O^-)(O_2)]^+$ and *trans*-μ-1,2-peroxo complex $\{[Cu(TMPA)_2](O_2)\}^{2+}$ have been tested for a variety of reactions as applied for $[Cu_2(N4PY2)(O_2)]^{2+}$. Both complexes exhibit comparable reactivities. They react with PPh_3 to give the corresponding copper(I) adduct; no formation of $OPPh_3$ was detected. Protonation of the complexes with HBF_4 or HPF_6 gives nearly stoichiometric yields of H_2O_2. The low-temperature reaction between 2,4-di-*tert*-butylphenol and $[Cu_2(XYL\text{-}O^-)(O_2)]^+$ results in the formation of the hydroperoxo complex $[Cu_2(XYL\text{-}O^-)(OOH)]^+$, and warming the solution gives a phenoxo complex. $\{[Cu(TMPA)]_2(O_2)\}^{2+}$ reacts with these substrates in a similar manner. Both complexes react with CO_2 and SO_2, affording μ-carbonato and μ-sulfato complexes. Together with the product distributions obtained in the reactions with Ph_3C^+ and $4\text{-}X\text{-}C_6H_4MgBr$ (X = Me, F), it was concluded that both peroxo complexes are nucleophilic. Thus, the reaction chemistry of these complexes essentially parallels that of planar $\mu\text{-}\eta^2{:}\eta^2$-peroxo complexes.

When the putative μ-peroxo complex $[Cu_2(1,2\text{-}Me_2im)_6(O_2)]^{2+}$ was treated with TMPA, $\{[Cu(TMPA)]_2(O_2)\}^{2+}$ was produced.[66] The addition of phosphines effected the liberation of dioxygen, yielding the corresponding copper(I)–phosphine complexes. While the complex reacted with protons to liberate hydrogen peroxide, treatment with CO_2 resulted in the formation of a carbonato complex $[Cu_2(1,2\text{-}Me_2im)_6(CO_3)]^{2+}$. These results suggest that the μ-peroxo complex is nucleophilic as well as $\{[Cu(TMPA)]_2(O_2)\}^{2+}$.[66]

3. Ligand Hydroxylations

A considerable number of ligand oxidations has been reported, where aerobic treatment of a copper(I) complex, mostly dinuclear, yields an isolable dinuclear copper(II) complex with an oxidized ligand. Representive examples are in eqs 15–17.[43,60,80] As described already, a dinuclear copper(I) complex $[Cu_2(UN)]^{2+}$ reacts with dioxygen at −80 °C, to form a relatively stable μ-peroxo complex $[Cu_2(UN)(O_2)]^{2+}$.[59] When the solution was warmed to room temperature, the aromatic ring was hydroxylated, affording a dinuclear copper(II) complex $[Cu_2(UN\text{-}O^-)(OH)]^{2+}$.[59] These observations imply strongly that the ligand hydroxylation proceeds via the μ-peroxo complex. The reaction mechanism of aerobic oxidation of $[Cu_2(XYL\text{-}H)]^{2+}$ to $[Cu_2(XYL\text{-}O^-)(OH)]^{2+}$ was studied in detail.[77] While

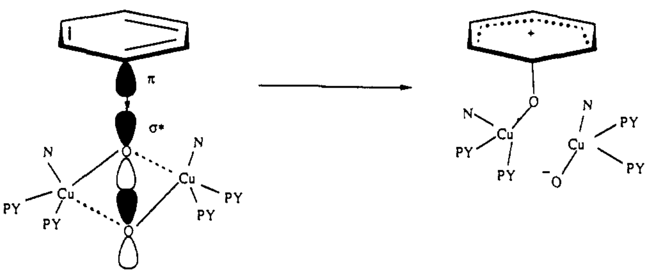

Figure 11. Electrophilic oxo insertion proposed for hydroxylation of $[Cu_2(XYL\text{-}H)]^{2+}$ via a bent μ-peroxo intermediate. (Reprinted from ref 77. Copyright 1992 American Chemical Society.)

the μ-peroxo intermediate could not be identified spectroscopically owing to its instability, on the basis of the closely related ligand structure to UN, it was demonstrated that the reaction proceeds via a μ-peroxo intermediate whose structure is similar to $[Cu(UN)(O_2)]^{2+}$. When a methyl group is introduced at the 1-position of the aromatic ring in the ligand, migration of the methyl group was noted during the ligand oxidation.[76] Since the reaction pattern is similar to the NIH shift, a mechanism is proposed which involves an electrophilic attack of a bent μ-η^2:η^2-peroxide to the CH bond of the aromatic ring as illustrated in Figure 11.[77]

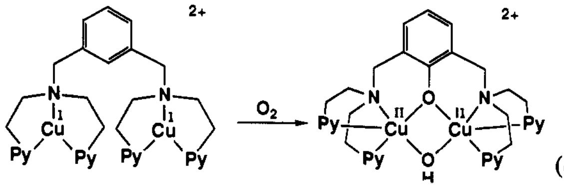

(eq 15)

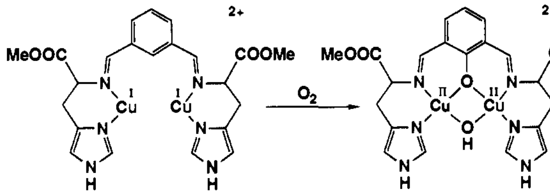

(eq 16)

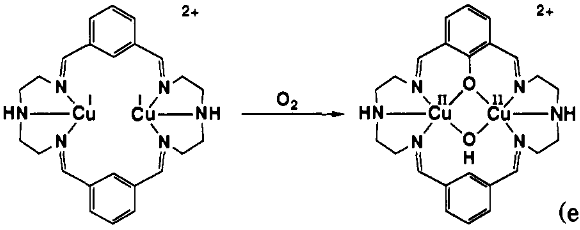

(eq 17)

Several examples of similar aromatic ligand hydroxylations and other types ligand oxidations including oxidative dehydrogenation of amines and aliphatic hydroxylation have been reported.[78-88] These reactions are also supposed to proceed via a μ-peroxo complex. However, the spectroscopic identification of the intermediate has not been accomplished in any of these systems, and the detailed mechanistic exploration remains to be undertaken.

V. Other Peroxo-Copper(II) Complexes

It is known that protonation and acylation of a peroxo transition metal complex lead to the formation of the corresponding hydroperoxo and acylperoxo complexes, respectively.[89-91] Protonation of $[Cu_2(XYL\text{-}O^-)(O_2)]^+$ at low temperature causes a color change of the solution from deep purple to green.[92] Whereas the original peroxo complex is not effective for oxidation of PPh_3 to $OPPh_3$, the protonated complex does. The protonated species also oxygenates tetrahydrothiophene to tetrahydrothiophene *S*-oxide, quantitatively. A detailed structural study mainly based on EXAFS suggested that the protonated species is a μ-1,1-hydroperoxo dinuclear copper(II) complex (eq 18).[92] The same species is also produced by dioxygen treatment of a dinuclear copper(I) complex in which a phenol group is attached as shown in eq 19. A similar protonation reaction to yield μ-1,1-hydroperoxo complex was found to occur for $[Cu_2(UN\text{-}O^-)(O_2)]^+$ as well.[46] The asymmetric dinucleating ligand UN-O⁻ enhances the thermal stability of the resultant hydroperoxo complex more than that of the complex with XYL-O⁻, and thus the hydroperoxo complex was successfully isolated as a solid. The acylation of $[Cu_2(XYL\text{-}O^-)(O_2)]^+$ with m-$ClC_6H_4C(O)Cl$ results in the formation of an acylperoxo complex $[Cu_2(XYL\text{-}O^-)(m\text{-}ClC_6H_4C(O)OO)]^{2+}$ which was also obtained by the reaction of μ-hydroxo complex $[Cu_2(XYL\text{-}O^-)(OH)]^{2+}$ with m-$ClC_6H_4C(O)OOH$.[93] The acylperoxo complex was isolated as crystals and structurally determined by X-ray crystallography, the ORTEP view being given in Figure 12. Consistent with the frequency (1745 cm^{-1}) of ν(CO) which is almost identical to that of free m-$C_6H_4C(O)OOH$, the acyl carbonyl group does not interact with the copper ion, and the coordination of the acylperoxo group is μ-1,1 as predicted for the hydroperoxo complex. While this is the first X-ray structure of an acylperoxo–transition metal complex, the O–O distance of 1.46 Å is typical for a peroxide bound to a transition metal ion found in other peroxo[15] or alkylperoxo complexes.[94-100] As well as the hydroperoxo complex, the acylperoxo dinuclear copper(II) complex is effective for oxo-transfer reactions to PPh_3 and tetrahydrothiophene. $[Cu_2(XYL\text{-}O^-)(O_2)]^+$ also reacts with EtOC(O)Cl and $(CF_3CO)_2O$ to form acylperoxo complexes and Et_3OPF_6 to produce an alkylperoxo complex.[74b] The formation of a hydroperoxo or an acylperoxo complex was also found when a *trans*-μ-1,2-peroxo complex $\{[Cu(TMPA)]_2(O_2)\}^{2+}$ was treated with proton or benzoyl chloride, but the details of the structure and reactivity of the complexes have not been reported.[74b]

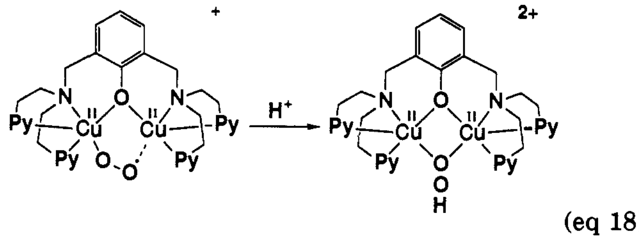

(eq 18)

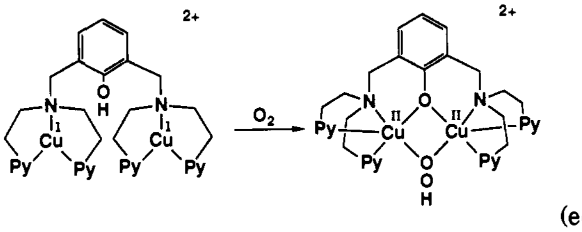

(eq 19)

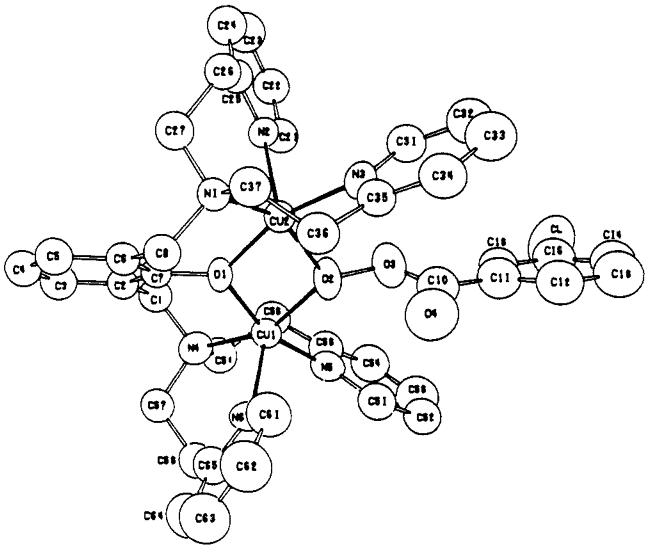

Figure 12. ORTEP view of $[Cu_2(OOC(O)C_6H_4\text{-}m\text{-}Cl)(XYL\text{-}O^-)]^{2+}$. The selected bond distances (Å) and angles (°) are as follows: Cu1···Cu2, 3.197; Cu1–O1, 1.948(8); Cu1–O2, 1.971(9); Cu2–O1, 1.959(8); Cu1–O2, 1.973(90); O2–O3, 1.463(12); Cu1–O1–Cu2, 109.8(3); Cu1–O2–Cu2, 108.3(4). (Reprinted from ref 93. Copyright 1987 American Chemical Society.)

The reaction of a bis(μ-hydroxo) dinuclear copper(II) complex $[Cu[HB(3,5\text{-}iPr_2pz)_3]]_2(OH)_2$ with 2 equiv of $m\text{-}ClC_6H_4C(O)OOH$ and ROOH gave monomeric acylperoxo- and alkylperoxo-copper(II) complex $Cu[m\text{-}C_6H_4C(O)OO][HB(3,5\text{-}iPr_2pz)_3]$ and $Cu(ROO)[HB(3,5\text{-}iPr_2pz)_3]$, respectively (eqs 20 and 21).

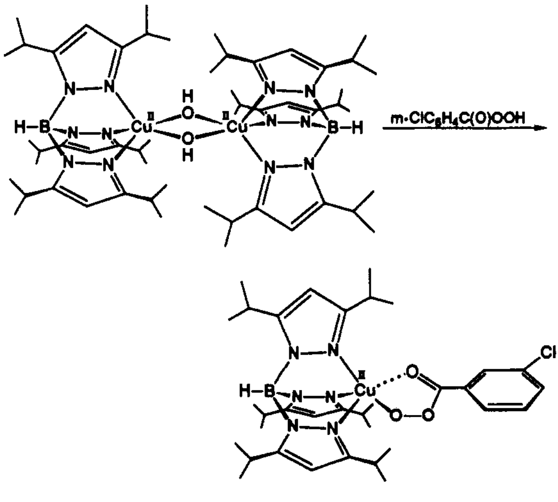

(eq 20)

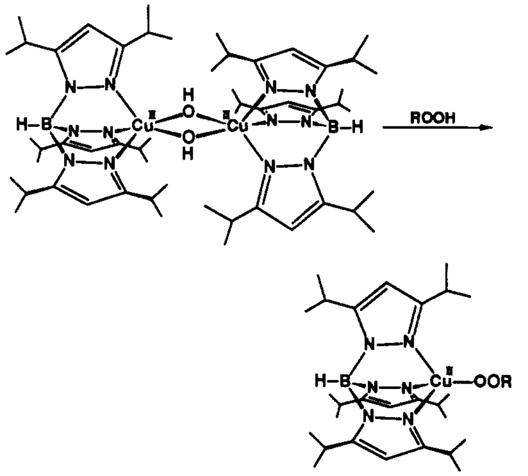

(eq 21)

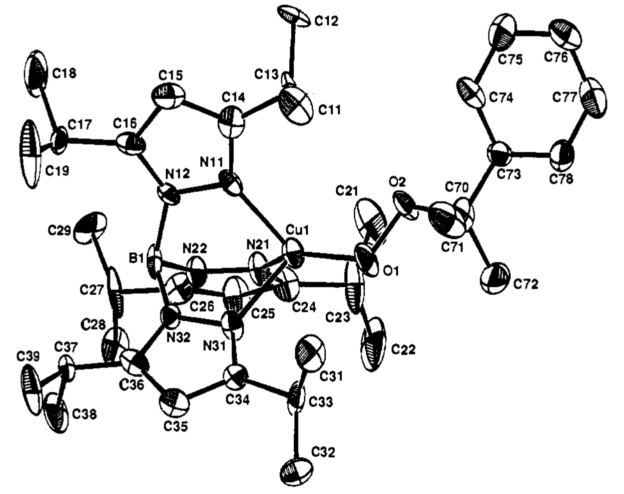

Figure 13. ORTEP view of $Cu(PhMe_2COO)[HB(3,5\text{-}iPr_2\text{-}pz)_3]$. The selected bond distances (Å) and angles (°) are as follows: Cu1–O1, 1.816(4); Cu1–N11, 1.982(6); Cu1–N21, 1.949(6); Cu1–N31, 2.161(6); O1–O2, 1.460(6); Cu1–O1–O2, 112.1(4). (Reprinted from ref 102. Copyright 1993 American Chemical Society.)

The monomeric five-coordinate structure of the thermally unstable acylperoxo complex with a bidentate coordination mode of the acylperoxo group was estimated on the basis of the IR and EPR spectrum. [ν(CO) is observed at 1640 cm^{-1} which is significantly down-shifted from that of free $m\text{-}C_6H_4C(O)OOH$.[101]] Although this complex reacts with PPh_3 instantaneously to afford $OPPh_3$ with formation of a monomeric benzoate complex $Cu(m\text{-}Cl\text{-}C_6H_4COO)[HB(3,5\text{-}iP_2\text{-}pz)_3]$, its oxidizing capability is not markedly high, being ineffective for epoxidation of cyclohexene. $Cu(PhMe_2COO)[HB(3,5\text{-}iPr_2pz)_3]$ was crystallized and its molecular structure was determined.[102] As shown in Figure 13, it adopts a distorted tetrahedral geometry with the mean O–O distance of 1.46 Å which is typical for such a bond.[94-100] Exploration of the reactivity of $Cu(tBuOO)[HB(3,5\text{-}iPr_2pz)_3]$ indicated that the alkylperoxo complex is not very effective for oxo-transfer reactions. The complex reacts only with substrates such as PPh_3 which are easily oxidized. The alkylperoxo complex is essentially nucleophilic, since it oxidizes tetrahydrothiophene *S*-oxide but not tetrahydrothiophene. When the oxidation reaction was carried out at room temperature, the complex undergoes spontaneous decomposition accompanied by the oxidation of solvent (pentane). The reaction with cyclohexene and pentane gave typical radical type reaction products such as dicyclohexenyl and butyl pentyl peroxide, suggesting that the oxidation reaction predominantly proceeds via classical type radical reactions initiated by $tBuOO^•$ which is generated by the reductive cleavage of the Cu–O bond of the alkylperoxo complex.

VI. Biological Relevance

A. Coordination Mode of the Peroxide in Oxyhemocyanin

Hemocyanin is a ubiquitous dioxygen carrier for invertebrates, containing a dinuclear copper site to which dioxygen is bound as peroxide.[7-9] The resonance Raman exploration with mixed labeled dioxygen established that the peroxide coordination is symmetric.[14]

Whereas the two copper ions are divalent in the dioxygen binding state (so-called oxyhemocyanin), oxyhemocyanin is EPR silent and in fact, diamagnetic at room temperature, due to an enormously strong antiferromagnetic coupling ($-2J > 600$ cm^{-1}) between the two cupric ions.[12,13] Furthermore, instead of d–d bands normally observed at 600–700 nm for cupric complexes, oxyhemocyanin exhibits two intense bands at ca. 350 (~20 000/2Cu) and ca. 580 (~1000), both attributable to $O_2^{2-} \rightarrow Cu(II)$ LMCT transitions. Other intriguing features of oxyhemocyanin associated with the $Cu^{II}–O_2^{2-}–Cu^{II}$ chromophore include the abnormally low ν(O–O) frequency (ca. 750 cm^{-1}) and a characteristic band at ca. 450 nm detected only in the CD spectrum.[7-9,103] In the generally accepted scenario, the existence of an endogenous bridging ligand was believed to be responsible for the strong magnetic interaction. On the basis of this interpretation, dioxygen was suggested to be bound at the dinuclear copper site in hemocyanin in a cis-coordination mode as schematically illustrated in eq 22.

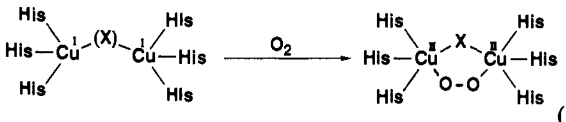

(eq 22)

As a most plausible candidate for the endogenous bridging ligand, tyrosine phenoxide was proposed previously; however, this possibility is now excluded since the 3.2-Å resolution X-ray analysis of the reduced state hemocyanin from a lobster (*Panulirus interruptus*) established that there is no amino acid residue within 6 Å from the dinuclear copper site where each cuprous ion was found to be surrounded by three histidyl nitrogen ligands.[104,105] Thus, another small ligand, most possibly hydroxide, has more recently been accepted as the endogenous bridging ligand.

Support for the *cis*-μ-1,2 coordination mode of the peroxide with an endogenous ligand mainly lies in the detailed spectroscopic studies performed by Solomon and co-workers on metazidohemocyanin which is prepared by azide ion treatment of oxyhemocyanin.[106-108] Because metazidohemocyanin is EPR silent as well as oxyhemocyanin, it was suggested that simple ligand displacement between the peroxide and azide occurs with preservation of the endogenous bridging ligand which is responsible for the strongly antiferromagnetic behavior. Azide ion has a π^{nb} HOMO which is very similar to the π^* valence level of peroxide. In analogy to peroxide, π^{nb} splits into π^{nb}_σ and π^{nb}_v when azide bridges between two cupric ions. Whereas the $\pi^{nb}_v \rightarrow$ Cu(II) LMCT band is too weak to be observed, the $\pi^{nb}_\sigma \rightarrow$ Cu(II) transition appears as an intense optical band, which splits further into two bands when the azide bridging mode is *cis*-μ-1,3 because of the transition dipole coupling.[108,109] The detailed comparison of the absorption spectrum of metazidohemocyanin with those of a series of dinuclear copper–azide model complexes led to a conclusion that the azide ion in metazidohemocyanin adopts a *cis*-μ-1,3 coordination mode with an endogenous bridging ligand, most likely hydroxide.[110] Since the azide ion favors the same coordination mode as does peroxide, this strongly supports the hypothesis that the peroxide coordination mode in oxyhemocyanin is a *cis*-μ-1,2 as indicated in eq 22. On the other hand, the possibility that oxyhemocyanin adopts a *trans*-μ-1,2 coordination mode of peroxide is excluded, because the properties of a model complex $\{[Cu(TMPA)]_2(O_2)\}^{2+}$, whose structure was determined by X-ray crystallography, do not fit with those of oxyhemocyanin as evidenced in Table 2.

The striking and unusual magnetic and spectral characteristics of oxyhemocyanin have fascinated many inorganic chemists, and the synthesis of a μ-peroxo–dicopper(II) complex modeling the active site of oxyhemocyanin has been a long-standing challenge in bioinorganic chemistry.[16-21,111-113] Despite extensive efforts, however, no synthetic complex that closely mimics the physicochemical characteristics of oxyhemocyanin had been known before the planar μ-η^2:η^2-peroxo complexes, $[Cu[HB(3,5-R_2pz)_3]]_2(O_2)$, were synthesized. This implies that the $Cu(O_2^{2-})Cu$ chromophore in oxyhemocyanin is structurally, and consequently spectroscopically unique among copper dioxygen complexes. Therefore, the remarkable similarities of the μ-η^2:η^2-peroxo complexes to oxyhemocyanin in their physicochemical characteristics including the Cu···Cu separation, magnetic property, UV–vis, and Raman spectra (see Table 2) have raised a new possibility that the peroxide coordination in oxyhemocyanin also adopts μ-η^2:η^2 without an additional bridging ligand.

The coordination mode of the peroxide in oxyhemocyanin has been generally believed to be a cis-μ-1,2 with an endogenous bridging ligand, most likely hydroxide as described already. However, the existence of the additional bridging ligand has not been proved experimentally, despite many spectroscopic investigations. Given the coordination mode of the peroxide as μ-η^2:η^2, it is not necessary to consider the hypothetical presence of the additional ligand other than the peroxide and thus the binding of dioxygen at the dinuclear copper site in hemocyanin is interpreted by a simple dioxygen addition as illustrated in eq 23.[16,33,112,113]

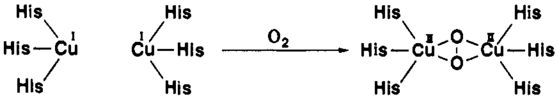

(eq 23)

Structural comparison of the $N_3Cu(O_2)CuN_3$ moiety in $[Cu[HB(3,5-iPr_2pz)_3]]_2(O_2)$ and the X-ray structure of deoxyhemocyanin from *P. interruptus*[104,105] supports this new binding model. Each cuprous ion in deoxyhemocyanin is surrounded by three histidyl nitrogen atoms from the protein chains, with the Cu···Cu separation of 3.54 Å.[105] The coordination structures of the two cuprous ions closely resemble each other; each consists of two short Cu–N bonds and a third distinctly elongated Cu–N bond. This feature is schematically indicated in Figure 14 as A. It is noteworthy that the four nitrogen and two cuprous ions proximately sit on the same plane and the two apical nitrogen atoms relate to each other in a trans configuration. All these structural features of the coordination environment of the dicopper site in dioxyhemocyanin are very close to the $N_3Cu(O_2)CuN_3$ moiety found in $[Cu[HB(3,5-iPr_2pz)_3]]_2(O_2)$ (see Figure 4), except for the longer Cu–N_{apical} distance in the protein. Accordingly, dioxygen would fit in the planar $N_2Cu–CuN_2$ frame in deoxyhemocyanin, without a serious structural change, re-

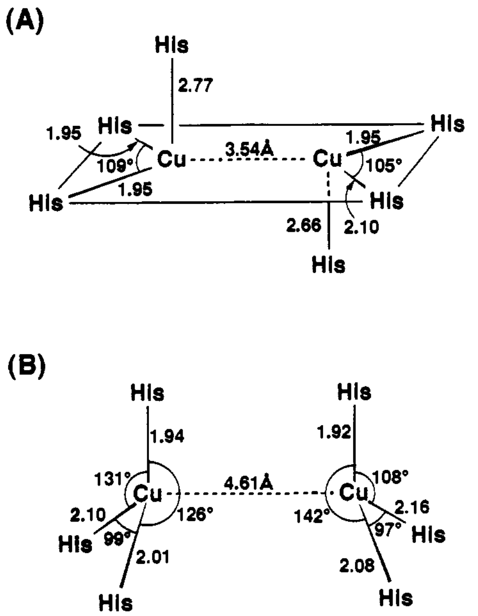

Figure 14. Schematic representation of the dinuclear copper site in deoxy hemocyanin: (A) *Panulirus interruptus* (from ref 105) and (B) *Limulus polyphemus* (from ref 114).

sulting in the peroxide binding in the μ-η^2:η^2 mode. Very recently, the crystal structure of *Limulus polyphemus* subunit type II hemocyanin in the deoxygenated state has been determined to a resolution of 2.18 Å.[114] The dinuclear copper site revealed in this protein has the structural features distinctive from that found in *Panulirus interruptus* deoxyhemocyanin; the Cu···Cu separation of 4.61 Å is much longer, and each copper coordination environment is nearly trigonal planar with Cu–N ligand distances between 1.92 and 2.16 Å. The schematic diagram of the copper site is presented as B in Figure 14. The unexpected long Cu···Cu separation found in *Limulus* deoxyhemocyanin suggested the requirement of a relatively large structural change when dioxygen is bound at this site. In fact, this was confirmed by X-ray structural determination of oxygenated state of the hemocyanin (vide infra).

The 2.4-Å resolution structure of oxyhemocyanin from *L. polyphemus* has been reported by Magnus et al. very recently, which confirmed that the peroxide is bridged between the two cupric ions in a planar μ-η^2:η^2 coordination mode but not in a *cis*-μ-1,2 with an additional bridging ligand.[115] The overall structural features of the $N_3Cu(O_2)CuN_3$ chromophore including the Cu···Cu separation of 3.6 Å and the O–O distance of 1.4 Å revealed in the oxyhemocyanin are very similar to those found in $[Cu[HB(3,5\text{-}iPr_2pz)_3]]_2(O_2)$.[33]

Given the coordination mode of the peroxide in oxyhemocyanin as μ-η^2:η^2, the question arises as to how the (μ-hydroxo)(μ-1,3-azido) bridge in metazidohemocyanin can be constructed from the μ-η^2:η^2-peroxo bridge by simple azide treatment of oxyhemocyanin. To address this question, the reaction of the model complex $[Cu(HB(3,5\text{-}iPr_2pz)_3)]_2(O_2)$ with azide was explored.[116] The reaction between the μ-η^2:η^2-peroxo complex and NaN_3/H_2O proceeded readily, resulting in formation of a dinuclear copper(II) complex containing a novel (μ-hydroxo)(μ-1,3-azido) bridge, the structure of which was established definitely by X-ray crystallography (eq 24).[116]

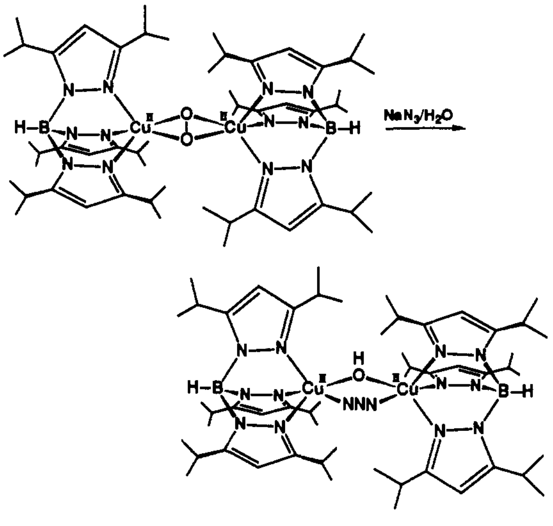

(eq 24)

Since the properties of the μ-azide complex including the Cu···Cu separation, magnetism, $\nu_{asym}(N_3)$, and UV–vis spectral features are similar to those known for metazidohemocyanin, the complex serves as an accurate synthetic analogue for the dinuclear copper site in metazidohemocyanin. The labeling experiment indicated that the bridging hydroxide originates from water. While the detailed mechanism remains to be solved, this notable transformation found in the small synthetic model complex suggested that the μ-η^2:η^2-peroxo bridge in oxyhemocyanin is converted into the (μ-hydroxo)(μ-1,3-azido) bridge in the presence of azide ion, where the hydroxide comes from water.

B. Mechanism of Tyrosinase

Tyrosinase is a monooxygenase which catalyzes the oxidation of phenol to benzoquinone. The active site

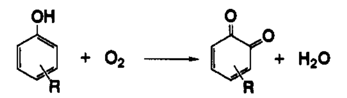

(eq 25)

of tyrosinase consists of a pair of copper ions, and the dioxygen adduct, so called oxytyrosinase, exhibits spectral features which closely resemble those of oxyhemocyanin (Table 2). Hence, the coordination mode of the peroxide in oxytyrosinase is reasonably suggested to be planar μ-η^2:η^2. The reaction of the model compound $[Cu[HB(3,5\text{-}Me_2pz)_3]]_2(O_2)$ and hindered phenols merely yields diphenoquinones but not benzoquinones. Since diphenoquinones are apparently radical reaction products, the formation of such products may be accepted as a negative indication for a tyrosinase reaction mimic. However, when phenols are hindered like those used for the model study, tyrosinase also gives diphenoquinones primarily.[117,118] Therefore, the reaction chemistry of $[Cu[HB(3,5\text{-}Me_2pz)_3]]_2(O_2)$ may provide mechanistic insight into the catalysis of tyrosinase. As described already, the anaerobic oxidation of phenols with $[Cu[HB(3,5\text{-}Me_2pz)_3]]_2(O_2)$ was proposed to proceed via phenoxo radical which is generated by two distinct reaction pathways. One is the spontaneous O–O bond cleavage of the peroxide to afford Cu(II)–O$^\bullet$ species which abstracts H$^\bullet$ from phenol. The other one is acid/base replacement between the acidic phenol and the basic peroxide to give a phenoxo intermediate which undergoes reductive

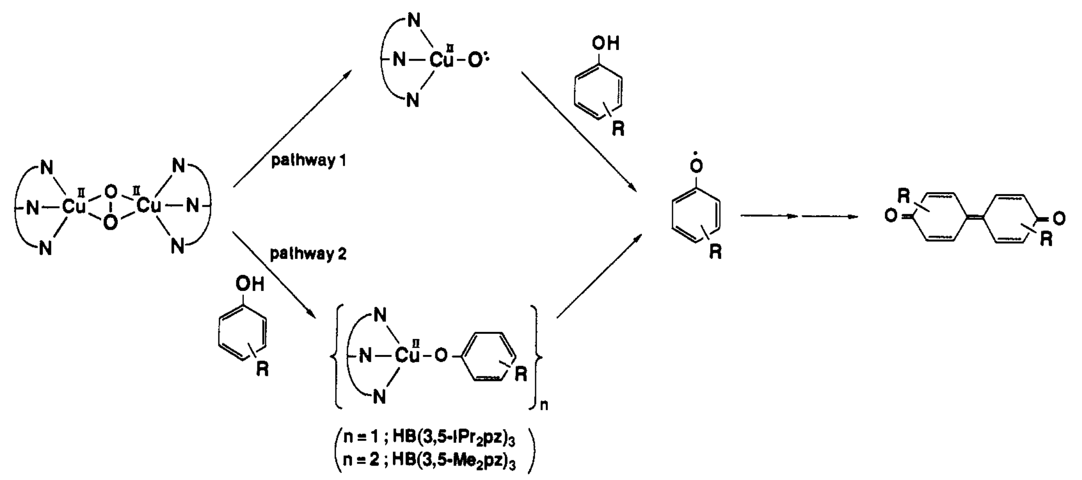

Figure 15. Mechanism of phenoxo radical formation in the reaction of a μ-η^2:η^2-peroxo–dicopper(II) complex with phenol. The phenoxo intermediate formed between $[Cu[HB(3,5\text{-}Me_2pz)_3]]_2(O_2)$ was suggested to have a dinuclear structure,[71] whereas the corresponding complex with $HB(3,5\text{-}iPr_2pz)_3$ is monomeric, whose structure was confirmed by X-ray crystallography, due to the more steric hindrance of the ligand.[73]

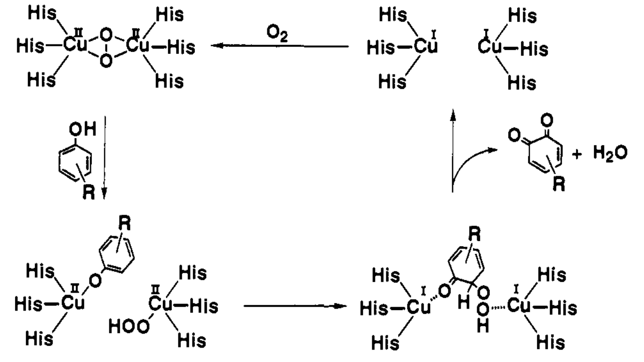

Figure 16. Proposed mechanism of tyrosinase catalysis (from ref 118).

Cu–O bond cleavage, resulting in formation of phenoxo radical (see Figure 15). O–O bond homolysis may not occur in tyrosinase if the two copper ions are held by the protein chains so as to reverse the cleavage. On the other hand, there is a high possibility that the latter type reaction to form a phenoxo intermediate does occur in the initial reaction step in the catalysis of tyrosinase. Presumably only one phenol molecule is accessible to the active site because of space limitations and formation of the phenoxo intermediate is suggested to cause formation of a hydroperoxo intermediate as shown in the mechanism of Figure 16. Unfortunately, the reaction chemistry of hydroperoxo copper complexes is scarcely known. However, in light of the reactivity of the alkylperoxo complex, $Cu(tBuOO)[HB(3,5\text{-}iPr_2pz)_3]$ described above,[102] it seems highly likely that the hydroperoxo intermediate undergoes Cu–O bond homolysis. In this case, it is reasonable to assume that the phenoxo radical and HOO• couple to each other instantaneously in the coordination sphere of the dinuclear copper site to give a hydroperoxybenzoquinone which is converted to benzoquinone, completing the catalytic cycle, as illustrated in Figure 16. The formation of hydroxylbenzoquinone may occur via a concerted mechanism, since the ortho position of the phenoxo group bound to cupric ion is activated to be susceptible to the radical coupling. This may be the most plausible mechanism for tyrosinase catalysis deduced from the model studies. When the phenol is hindered, the inner-sphere coupling between the phenoxide and hydroperoxide does not occur effectively and thus the phenoxo radical is released from the active site to give the diphenoquinone via free radical mechanism.

On the other hand, there is another possible mechanism which involves a direct electrophilic attack of the μ-η^2:η^2-peroxide to the CH bond of the phenol as demonstrated by Karlin et al. for the mechanism of the aerobic arene hydroxylation of copper(I) complexes. The SCF-Xα calculations[38] have indicated that the μ-η^2:η^2 is less negative than other peroxide coordination modes, such as *trans*-μ-1,2 and terminal ones, because the π_σ* electron interacts with the copper d orbital more strongly than with the others. In addition, the peroxide σ* orbital works as a π acid when the coordination mode of the peroxide is μ-η^2:η^2. If the peroxide O–O bond aligns its empty σ* orbital with the π–π orbital of the phenol, the electrophilic attack and the following O–O bond cleavage is predicted to be facilitated. Since a considerable number of ligand hydroxylations are now known, this possibility should be taken into account in considering the mechanism of tyrosinase. However, as described already, in none of these ligand hydroxylation reactions, has the identification of the μ-peroxo intermediate been credibly accomplished. Moreover, all of these systems are ineffective for oxo-transfer reactions of externally added substrates. Thus, the hypothesis that the putative μ-η^2:η^2-peroxo intermediate is electrophilic so as to incorporate oxygen into CH bond of phenol directly remains to be proved. Consequently, there are two possible reaction mechanisms for tyrosinase in which a μ-η^2:η^2-peroxo species is a key reaction intermediate. One is the mechanism involving initial formation of a phenoxo hydroperoxo intermediate followed by a radical type oxidation. The other is the direct electrophilic insertion of peroxide oxygen into CH bond of tyrosine. Clearly, more extensive investigation on the reactivity of μ-peroxo (particularly μ-η^2:η^2) complex is necessary to lead to a conclusive catalytic mechanism of tyrosinase.

C. Future Perspectives

As described above, the synthesis and structural characterization of μ-η^2:η^2-peroxo dinuclear copper complexes have provided insight into the detailed coordination structure of the peroxide in hemocyanin and tyrosinase. The reaction chemistry of the complex has also shed light on new facets of the reaction mechanism of tyrosinase. However, a unified view of the reactivity of peroxo–copper complexes has not been achieved. A number of questions remain to be answered; for example, are these complexes highly reactive or not, electrophilic or nucleophilic? The reactivity probably depends on many structural factors including the coordination mode of the peroxide, coordination geometry and ligand donor set around the copper, and availability of a reaction site with a the proper orientation to facilitate the oxo-transfer reaction to the substrate. More extensive explorations on peroxo–copper complexes not only of μ-η^2:η^2 but also of other structural types are apparently necessary for a better understanding of the reaction mechanism of tyrosinase, which should also shed light on the functional role of the copper ion in some other copper monooxygenases.

Several monooxygenases containing a monomeric copper site are known and are listed in Table 1. The credible characterization of monomeric superoxo– or peroxo–copper complexes and their reaction chemistry is a clear direction for future studies. These studies may also be relevant to other copper-containing oxidases such as amine oxidase[119] and galactose oxidase[120] whose active site is monomeric and the direct interaction between the copper and dioxygen is possibly involved. Very recently, a methane monooxygenase from *Methylococcus capsulatus* (Bath) was found to contain copper ions.[121] On the basis of analytical and spectroscopic results, this particular enzyme is suggested to contain a novel exchange-coupled trinuclear copper cluster as its active site. While the magnetic property is distinctive, an isosceles triangle shaped trinuclear copper site is already known to be present in laccase[122] and ascorbate oxidase.[123] Dioxygen is presumably bound and activated at the trinuclear copper site. The synthesis and characterization of a trinuclear copper dioxygen complexes is a significant challenge to biological inorganic chemists.

Copper dioxygen complexes are supposed to play crucial roles in other metalloproteins as well. Cytochrome *c* oxidase, a key enzyme in respiration, contains a hetero-bimetallic active site consisting of a copper and a heme.[124] The four-electron reduction of dioxygen to water catalyzed by this enzyme may proceed via a peroxo bridged copper/heme intermediate,[125] while another possibility that copper does not participate in dioxygen binding has been put forth.[126] Initial attempts to synthesize this type of complex have emerged.[127,128] Another notable enzyme that may involve a copper dioxygen species is Cu,Zn superoxide dismutase.[129] It is generally accepted that the zinc ion in this enzyme which is connected to the copper through a bridging imidazolate group is required as a structural template, and copper but not zinc is responsible for binding of superoxide. A hetero-dinuclear copper/zinc dioxygen complex is an intriguing synthetic analogue of the enzymatic intermediate, whose chemistry may shed new light on the mechanism of this physiologically important reaction.

VII. Abbreviations

EXAFS	extended X-ray absorption fine structure
XANES	X-ray absorption near-edge structure
XAS	X-ray absorption spectroscopy
XPS	X-ray photoelectron spectroscopy
LMCT	ligand-to-metal charge transfer
FD-MS	field desorption mass spectroscopy
SCF-Xα-SW	self-consistent field-Xα-scattered wave
tetb	*rac*-5,7,7,12,14,14-hexamethyl-1,4,8,11-tetraazacyclotetradecane
HB(3,5-$Me_2pz)_3$	hydrotris(3,5-dimethyl-1-pyrazolyl)borate
HB(3,5-$Ph_2pz)_3$	hydrotris(3,5-diphenyl-1-pyrazolyl)borate
HB(3,5-$iPr_2pz)_3$	hydrotris(3,5-diisopropyl-1-pyrazolyl)borate
TMPA	tris[(2-pyridyl)methyl]amine
BPQA	bis[(2-pyridyl)methyl][2-quinolyl)methyl]amine
BQPA	bis[(2-quinolyl)methyl][2-pyridyl)methyl]amine
TMQA	tris[(2-quinolyl)methyl]amine
Cyb	[bis[*N*,*N*-bis[(2-benzimidazolyl)methyl]amino]methyl]cyclohexane
XYL-H	α,α'-bis[*N*,*N*-bis[2-(2-pyridyl)ethyl]amino]-*m*-xylene
XYL-Cl	α,α'-bis[*N*,*N*-bis[2-(2-pyridyl)ethyl]amino]-2-chloro-*m*-xylene
XYL-O^-	α,α'-bis[*N*,*N*-bis[2-(2-pyridyl)ethyl]amino]-*m*-xylen-2-olate
UN	2-[[*N*,*N*-bis[2-(2-pyridyl)ethyl]amino]methyl]-6-[*N*,*N*-bis[2-(2-pyridyl)ethyl]amino]benzene
UN-O^-	2-[[*N*,*N*-bis[2-(2-pyridyl)ethyl]amino]methyl]-6-[*N*,*N*-bis[2-(2-pyridyl)ethyl]amino]phenolate
N4PY2	1,4-bis[*N*,*N*-bis[2-(2-pyridyl)ethyl]amino]butane
$MX_2(DIEN)_2$	3,6,9,17,20,23-hexaazatricyclo[23.3.1.$1^{11,15}$]triaconta-1(29),2,9,11(30),12(13),14,16,23,25,27-decaene
$(FD)_2(DIEN)_2$	3,6,9,16,19,22-hexaazatricyclo[22.2.1.$1^{11,14}$]octacosa-1(26),2,9,11,13,15,22,24-octaene
PhPY2	*N*,*N*-bis[2-(2-pyridyl)ethyl]·*N*-phenylamine
CH_3PY2	*N*,*N*-bis[2-(2-pyridyl)ethyl]-*N*-methylamine
$PhCH_2PY2$	*N*,*N*-bis[2-(2-pyridyl)ethyl]-*N*-benzylamine
$Bz(NMI)_2N3$	*N*,*N*-bis[2-(1′-methyl-2′-imidazolyl)ethyl]-*N*-benzylamine
$Bz(NBzI)_2N3$	*N*,*N*-bis[2-(1′-benzyl-2′-imidazolyl)ethyl]-*N*-benzylamine
1,2-Me_2Im	1,2-dimethylimidazole
BPIA	bis[(2-pyridyl)methyl][[2-(1-methylimidazolyl)]methyl]amine
BIPA	bis[[2-(1-methylimidazolyl)]methyl][(2-pyridyl)methyl]amine
N_4-MePY	bis[(2-pyridyl)methyl][6-methyl-2-pyridyl)methyl]amine
N_4-Me_2PY	bis[(6-methyl-2-pyridyl)methyl][(2-pyridyl)methyl]amine
tmpc	1,4,8,11-tetrakis[(2′-pyridyl)methyl]-1,4,8,11-tetraazacyclotetradecane
N30R	*N*,*N*,*N*′,*N*′-tetrakis[(2-pyridyl)methyl]-1,3-diaminoprop-2-yl biphenylcarboxylate
PhIO	iodosobenzene
OC_6H_4-*p*-F	*p*-fluorophenolate
m-ClC_6H_4-C(O)OOH	3-chloroperoxybenzoic acid
EtOC(O)Cl	ethyl chloroformate

$(CF_3CO)_2O$	trifluoroacetic anhydride
Et_3OPF_6	triethyloxonium hexafluorophosphate
$PhMe_2COOH$	cumene hydroperoxide

VIII. Acknowledgments

We thank S. Hikichi for the artwork for this review. We also thank Professor M. Suzuki, Dr. M. J. Baldwin, and Professor K. D. Karlin for valuable input. Financial support by a Grant-in-Aid for Scientific Research from the Japanese Ministry of Education, Science and Culture (04225107 and 04453044) is gratefully acknowledged.

IX. References

(1) Finkbeiner, H. L.; Hay, A. S.; White, D. M. *Polymerization Processes*; Schildknecht, C. E., Skeist, I., Eds.; Wiley-Interscience: New York, 1977; pp 537.

(2) Parshall, G. W. *Homogeneous Ctalysis*; Wiley-Interscience: New York, 1980; p 113.

(3) (a) Henry, P. M. *Adv. Organomet. Chem.* **1975**, *13*, 363. (b) Stern, E. W. *Catal. Rev.* **1968**, *1*, 74.

(4) (a) Cadiot, P.; Chodkiewicz, W. *Chemistry of Acetylenes*; Viehe, H. G., Ed.; Marcel Dekker: New York, 1969; p 597. (b) Hay, A. S. *J. Org. Chem.* **1962**, *27*, 3320.

(5) Rogic, M. M.; Demmin, T. R. *J. Am. Chem. Soc.* **1978**, *100*, 5472.

(6) Kaeding, W. W. *Hydrocarbon Proc.* **1964**, *43*, 173.

(7) *Structure and Function of Hemocyanin*; Bannister, J. V., Ed.; Springer-Verlag: Berlin, 1977.

(8) Solomon, E. I.; Penfield, K. W.; Wilcox, D. E. *Struct. Bonding (Berlin)* **1983**, *53*, 1.

(9) Solomon, E. I.; Baldwin, M. J.; Lowery, M. *Chem. Rev.* **1992**, *92*, 521.

(10) (a) Brown, J. M.; Powers, L.; Kincard, B.; Larrabee, J. A.; Spiro, T. G. *J. Am. Chem. Soc.* **1980**, *102*, 4210. (b) Woolery, G. L.; Powers, L.; Winkler, M.; Solomon, E. I.; Spiro, T. G. *J. Am. Chem. Soc.* **1984**, *106*, 86.

(11) Co, M. S.; Hodgson, K. O.; Eccles, T. K.; Lontie, R. *J. Am. Chem. Soc.* **1981**, *103*, 984.

(12) Moss, T. H.; Gould, D. C.; Ehrenberg, A.; Loehr, J. S.; Mason, H. S. *Biochemistry* **1973**, *12*, 2444.

(13) (a) Solomon, E. I.; Dooley, D. M.; Wang, R. H.; Gray, H. B.; Cerdonio, M.; Mogno, F.; Romani, G. L. *J. Am. Chem. Soc.* **1976**, *98*, 1029. (b) Dooley, D. M.; Scott, R. A.; Ellinghaus, J.; Solomon, E. I.; Gray, H. B. *Proc. Natl. Acad. Sci. U.S.A.* **1978**, *75*, 3019.

(14) (a) Freedman, T. B.; Loehr, J. S.; Loehr, T. M. *J. Am. Chem. Soc.* **1976**, *98*, 2809. (b) Thamann, T. J.; Loehr, J. S.; Loehr, T. M. *J. Am. Chem. Soc.* **1977**, *99*, 4187.

(15) Gubelman, M. H.; Williams, A. F. *Struct. Bonding (Berlin)* **1983**, *55*, 1.

(16) Kitajima, N. *Adv. Inorg. Chem.* **1992**, *39*, 1.

(17) Karlin, K. D.; Tyeklar, Z.; Zuberbühler, A. D. *Bioinorganic Catalysis*; Reedijk, J., Ed.; Marcel Dekker, Inc.: New York, 1993; Chapter 9, pp 261.

(18) Sorrell, T. N. *Tetrahedron* **1989**, *45*, 3.

(19) (a) *Biological & Inorganic Copper Chemistry*; Karlin, K. D., Zubieta, J., Eds.; Adenine Press: Guilderland, NY, 1986; Vols. 1 and 2. (b) *Copper Coordination Chemistry: Biochemical and Inorganic Perspectives*; Karlin, K. D., Zubieta, J., Eds.; Adenine Press: Gulderland, NY, 1983.

(20) Karlin, K. D.; Gultneh, Y. *Proc. Inorg. Chem.* **1987**, *35*, 219.

(21) Karlin, K. D.; Tyeklar, Z. *Adv. Inorg. Biochem.* **1993**, *9*, 123.

(22) Patterson, G. S.; Holm, R. H. *J. Bioinorg. Chem.* **1975**, *4*, 257.

(23) Hamilton, G. A.; Adolf, P. K.; de Jersey, J.; DuBois, G. C.; Dyrkacz, G. R.; Libby, R. D. *J. Am. Chem. Soc.* **1978**, *100*, 1899.

(24) (a) Whittaker, M. M.; Whittaker, J. W. *J. Biol. Chem.* **1988**, *263*, 6074. (b) Whittaker, M. M.; DeVito, V. L.; Asher, S. A.; Whittaker, J. W. *J. Biol. Chem.* **1989**, *264*, 7104.

(25) Nappa, M.; Valentine, J. S.; Miksztal, A. R.; Schugar, H. J.; Isied, S. S. *J. Am. Chem. Soc.* **1979**, *101*, 7744.

(26) Thompson, J. S. *J. Am. Chem. Soc.* **1984**, *106*, 4057.

(27) (a) Karlin, K. D.; Wei, N.; Jung, B.; Kaderli, S.; Zuberbühler, A. D. *J. Am. Chem. Soc.* **1991**, *113*, 5868. (b) Karlin, K. D.; Wei, N.; Jung, B.; Kaderli, S.; Zuberbühler, A. D. *J. Am. Chem. Soc.* **1993**, *115*, 9506.

(28) Mahroof-Tahir, M.; Karlin, K. D. *J. Am. Chem. Soc.* **1992**, *114*, 7599.

(29) (a) Jacobson, R. R.; Tyeklar, Z.; Farooq, A.; Karlin, K. D.; Liu, S.; Zubieta, J. *J. Am. Chem. Soc.* **1988**, *110*, 3690. (b) Tyeklar, Z.; Jacobson, R. R.; Wei, N.; Murthy, N. N.; Zubieta, J.; Karlin, K. D. *J. Am. Chem. Soc.* **1993**, *115*, 2677.

(30) Karlin, K. D.; Tyeklar, Z.; Farooq, A.; Jacobson, R. R.; Sinn, E.; Lee, D. W.; Bradshaw, J. E.; Wilson, L. J. *Inorg. Chim. Acta* **1991**, *182*, 1.

(31) Baldwin, M. J.; Ross, P. K.; Pate, J. E.; Tyeklar, Z.; Karlin, K. D.; Solomon, E. I. *J. Am. Chem. Soc.* **1991**, *113*, 8671.

(32) (a) Kitajima, N.; Koda, T.; Moro-oka, Y. *Chem. Lett.* **1988**, 347. (b) Kitajima, N.; Koda, T.; Hashimoto, S.; Kitagawa, T.; Moro-oka, Y. *J. Chem. Soc., Chem. Commun.* **1988**, 151. (c) Kitajima, N.; Koda, T.; Hashimoto, S.; Kitagawa, T.; Moro-oka, Y. *J. Am. Chem. Soc.* **1991**, *113*, 5664.

(33) (a) Kitajima, N.; Fujisawa, K.; Moro-oka, Y.; Toriumi, K. *J. Am. Chem. Soc.* **1989**, *111*, 8975. (b) Kitajima, N.; Fujisawa, K.; Fujimoto, C.; Moro-oka, Y.; Hashimoto, S.; Kitagawa, T.; Toriumi, K.; Tatsumi, K.; Nakamura, A. *J. Am. Chem. Soc.* **1992**, *114*, 1277.

(34) Bradley, D. C.; Ghotra, J. S.; Hart, F. A.; Hursthouse, M. B.; Raithby, P. R. *J. Chem. Soc., Dalton Trans.* **1977**, 1166.

(35) Haegele, R.; Boeyens, J. C. A. *J. Chem. Soc., Dalton Trans.* **1977**, 648.

(36) Lapsin, A. E.; Smolin, Y. J.; Shepelev, Y. F. *Acta Crystallogr.* **1990**, *C46*, 1755.

(37) Baldwin, M. J.; Root, D. E.; Pate, J. E.; Fujisawa, K.; Kitajima, N.; Solomon, E. I. *J. Am. Chem. Soc.* **1992**, *114*, 10421.

(38) (a) Ross, P. K.; Solomon, E. I. *J. Am. Chem. Soc.* **1990**, *112*, 5871. (b) Ross, P. K.; Solomon, E. I. *J. Am. Chem. Soc.* **1991**, *113*, 3246.

(39) Maddaluno, J.; Giessner-Prettre, C. *J. Am. Chem. Soc.* **1991**, *30*, 3439.

(40) (a) Karlin, K. D.; Cruse, R. W.; Gultneh, Y.; Hayes, J. C.; Zubieta, J. *J. Am. Chem. Soc.* **1984**, *106*, 3372. (b) Karlin, K. D.; Cruse, R. W.; Gultneh, Y.; Farooq, A.; Hayes, J.; Zubieta, J. *J. Am. Chem. Soc.* **1987**, *109*, 2668.

(41) Pate, J. E.; Cruse, R. W.; Karlin, K. D.; Solomon, E. I. *J. Am. Chem. Soc.* **1987**, *109*, 2624.

(42) Blackburn, N. J.; Strange, R. W.; Cruse, R. W.; Karlin, K. D. *J. Am. Chem. Soc.* **1987**, *109*, 1235.

(43) (a) Karlin, K. D.; Dahlstrom, P. L.; Cozzette, S. N.; Scensny, P. M.; Zubieta, J. *J. Chem. Soc., Chem. Commun.* **1981**, 881. (b) Karlin, K. D.; Hayes, J. C.; Gultneh, Y.; Cruse, R. W.; McKown, J. W.; Hutchinson, J. P.; Zubieta, J. *J. Am. Chem. Soc.* **1984**, *106*, 2121.

(44) Sorrell, T. N.; Jameson, D. L.; O'Connor, C. J. *Inorg. Chem.* **1984**, *23*, 190.

(45) Sorrell, T. N.; Vankai, V. A. *Inorg. Chem.* **1990**, *29*, 1687.

(46) Mahroof-Tahir, M.; Murthy, N. N.; Karlin, K. D.; Blackburn, N. J.; Shaikh, S. N.; Zubieta, J. *Inorg. Chem.* **1992**, *31*, 3001.

(47) Bulkowski, J. E.; Burk, P. L.; Ludmann, M.-F.; Osborn, J. A. *J. Chem. Soc., Chem. Commun.* **1977**, 498.

(48) Simmons, M. G.; Wilson, L. J. *J. Chem. Soc., Chem. Commun.* **1978**, 634.

(49) Youinou, M.-T.; Osborn, J. A.; Lagrange, P. *Inorg. Chem.* **1986**, *25*, 453.

(50) Merrill, C. L.; Wilson, L. J.; Thamann, T. J.; Loehr, T. M.; Ferris, N. S.; Woodruff, W. H. *J. Chem. Soc., Dalton Trans.* **1984**, 2207.

(51) Goodwin, J. A.; Bodager, G. A.; Wilson, L. J.; Stanbury, D. M.; Scheidt, W. R. *Inorg. Chem.* **1989**, *28*, 35.

(52) Nishida, Y.; Takahashi, K.; Kuramoto, H.; Kida, S. *Inorg. Chim. Acta* **1981**, *54*, L103.

(53) (a) Karlin, K. D.; Haka, M. S.; Cruse, R. W.; Gultneh, Y. *J. Am. Chem. Soc.* **1985**, *107*, 5828. (b) Karlin, K. D.; Haka, M. S.; Cruse, R. W.; Meyer, G. J.; Farooq, A.; Gultneh, Y.; Hayes, J. C.; Zubieta, J. *J. Am. Chem. Soc.* **1988**, *110*, 1196.

(54) Blackburn, N. J.; Strange, R. W.; Farooq, A.; Haka, M. S.; Karlin, K. D. *J. Am. Chem. Soc.* **1988**, *110*, 4263.

(55) Karlin, K. D.; Tyeklar, Z.; Farooq, A.; Haka, M. S.; Ghosh, P.; Cruse, R. W.; Gultneh, Y.; Hayes, J. C.; Toscano, P. J.; Zubieta, J. *Inorg. Chem.* **1992**, *31*, 1436.

(56) Karlin, K. D.; Gultneh, Y.; Hutchinson, J. P.; Zubieta, J. *J. Am. Chem. Soc.* **1982**, *104*, 5240.

(57) Karlin, K. D.; Cruse, R. W.; Haka, M. S.; Gultneh, Y.; Cohen, B. I. *Inorg. Chim. Acta* **1986**, *125*, L43.

(58) Nasir, M. S.; Cohen, B. I.; Karlin, K. D. *Inorg. Chim. Acta* **1990**, *176*, 185.

(59) Nasir, M. S.; Karlin, K. D.; McGowty, D.; Zubieta, J. *J. Am. Chem. Soc.* **1991**, *113*, 698.

(60) (a) Menif, R.; Martell, A. E. *J. Chem. Soc., Chem. Commun.* **1989**, 1521. (b) Menif, R.; Martell, A. E.; Squattrito, P. J.; Clearfield, A. *Inorg. Chem.* **1990**, *29*, 4723.

(61) Ngwenya, M. P.; Chen, D.; Martell, A. E.; Reibenspies, J. *Inorg. Chem.* **1991**, *30*, 2732.

(62) Sanyal, I.; Mahroof-Tahir, M.; Nasir, M. S.; Ghosh, P.; Cohen, B. I.; Gultneh, Y.; Cruse, R. W.; Farooq, A.; Karlin, K. D.; Liu, S.; Zubieta, J. *Inorg. Chem.* **1992**, *31*, 4322.

(63) Sorrell, T. N.; Garrity, M. L. *Inorg. Chem.* **1991**, *30*, 210.

(64) Suzuki, M. Personal communication.

(65) Sanyal, I.; Strange, R. W.; Blackburn, N. J.; Karlin, K. D. *J. Am. Chem. Soc.* **1991**, *113*, 4692.

(66) Sanyal, I.; Karlin, K. D.; Strange, R. W.; Blackburn, N. J. *J. Am. Chem. Soc.* **1993**, *115*, 11259.

(67) Wei, N.; Murthy, N. N.; Chen, Q.; Zubieta, J.; Karlin, K. D. *J. Am. Chem. Soc.*, submitted for publication.

(68) Wei, N.; Murthy, N. N.; Tyeklar, Z.; Karlin, K. D. *Inorg. Chem.*, in press.

(69) Uozumi, K.; Hayashi, Y.; Suzuki, M.; Uehara, A. *Chem. Lett.* **1993**, 963.

(70) Asato, E.; Hashimoto, S.; Matsumoto, N.; Kida, S. *J. Chem. Soc., Dalton Trans.* **1990**, 1741.

(71) Kitajima, N.; Koda, T.; Iwata, Y.; Moro-oka, Y. *J. Am. Chem. Soc.* **1990**, *112*, 8833.

(72) Chin, D.-H.; La Mar, G. N.; Balch, A. L. *J. Am. Chem. Soc.* **1980**, *102*, 4344.

(73) Kitajima, N.; et al. Manuscript in preparation.

(74) (a) Tyeklar, Z.; Paul, P. P.; Jacobson, R. R.; Farooq, A.; Karlin, K. D.; Zubieta, J. *J. Am. Chem. Soc.* **1989**, *111*, 388. (b) Paul, P. P.; Tyeklar, Z.; Jacobson, R. R.; Karlin, K. D. *J. Am. Chem. Soc.* **1991**, *113*, 5323.

(75) (a) Rockcliffe, D. A.; Martell, A. E. *J. Chem. Soc., Chem. Commun.* **1992**, 1758. (b) Rockcliffe, D. A.; Martell, A. E. *Inorg. Chem.* **1993**, *32*, 3143.

(76) Karlin, K. D.; Cohen, B. I.; Jacobson, R. R.; Zubieta, J. *J. Am. Chem. Soc.* **1987**, *109*, 6194.

(77) Nasir, N. S.; Cohen, B. I.; Karlin, K. D. *J. Am. Chem. Soc.* **1992**, *114*, 2482.

(78) Gagne, R. R.; Gall, R. S.; Lisensky, G. C.; March, R. E.; Speltz, L. M. *Inorg. Chem.* **1979**, *18*, 771.

(79) Thompson, J. S. *J. Am. Chem. Soc.* **1984**, *106*, 8308.

(80) (a) Casella, L.; Rigoni, L. *J. Chem. Soc., Chem. Commun.* **1985**, 1668. (b) Casella, L.; Gullotti, M.; Pallanza, G.; Rigoni, L. *J. Am. Chem. Soc.* **1988**, *110*, 4221.

(81) Patch, M. G.; McKee, V.; Reed, C. A. *Inorg. Chem.* **1987**, *26*, 776.

(82) Gelling, O. J.; van Bolhuis, F.; Meetsma, A.; Feringa, B. L. *J. Chem. Soc., Chem. Commun.* **1988**, 552.

(83) Reglier, M.; Amadei, E.; Tadayoni, R.; Waegell, B. *J. Chem. Soc., Chem. Commun.* **1989**, 447.

(84) Karlin, K. D.; Gan, Q.-F.; Farooq, A.; Liu, S.; Zubieta, J. *Inorg. Chem.* **1990**, *29*, 2549.

(85) Gelling, O. J.; Meetsma, A.; Feringa, B. L. *Inorg. Chem.* **1990**, *29*, 2816.

(86) Casella, L.; Gullotti, M.; Bartosek, M.; Pallanza, G.; Laurenti, E. *J. Chem. Soc., Chem. Commun.* **1991**, 1235.

(87) Sorrell, T. N.; Vankai, V. A.; Garrity, M. L. *Inorg. Chem.* **1991**, *30*, 207.

(88) Amadei, E.; Alilou, E. H.; Eydoux, F.; Pierrot, M.; Reglier, M.; Waegell, B. *J. Chem. Soc., Chem. Commun.* **1992**, 1782.

(89) Suzuki, H.; Matsuura, S.; Moro-oka, Y.; Ikawa, T. *J. Organomet. Chem.* **1985**, *286*, 247.

(90) Thewalt, U.; Marsh, R. E. *J. Am. Chem. Soc.* **1967**, *89*, 6364.

(91) Chen, M. J. K.; Kochi, J. K. *J. Chem. Soc., Chem. Commun.* **1977**, 204.

(92) (a) Karlin, K. D.; Cruse, R. W.; Gultneh, Y. *J. Chem. Soc., Chem. Commun.* **1987**, 599. (b) Karlin, K. D.; Ghosh, P.; Cruse, R. W.; Farooq, A.; Gultneh, Y.; Jacobson, R. R.; Blackburn, N. J.; Strange, R. W.; Zubieta, J. *J. Am. Chem. Soc.* **1988**, *110*, 6769.

(93) Ghosh, P.; Tyeklar, Z.; Karlin, K. D.; Jacobson, R. R.; Zubieta, J. *J. Am. Chem. Soc.* **1987**, *109*, 6889.

(94) Strukul, G.; Ros, R.; Michelin, R. A. *Inorg. Chem.* **1982**, *21*, 495.

(95) Mimoun, H.; Charpentier, R.; Mitschler, A.; Fischer, J.; Weiss, R. *J. Am. Chem. Soc.* **1980**, *102*, 1047.

(96) Nishinaga, A.; Tomita, H.; Nishizawa, K.; Matsuura, T.; Ooi, S.; Hirotsu, K. *J. Chem. Soc., Dalton Trans.* **1981**, 1504.

(97) Mimoun, H.; Chaumette, P.; Mignard, M.; Saussine, L.; Fisher, J.; Weiss, R. *Nouv. J. Chim.* **1983**, *7*, 467.

(98) Ferguson, G.; Monaghan, P. K.; Parvez, M.; Puddephatt, R. J. *Organometallics* **1985**, *4*, 1669.

(99) Saussine, L.; Brazi, E.; Robine, A.; Mimoun, H.; Fischer, J.; Weiss, R. *J. Am. Chem. Soc.* **1985**, *107*, 3534.

(100) van Asselt, A.; Santarsiero, B. D.; Bercaw, J. E. *J. Am. Chem. Soc.* **1986**, *108*, 8291.

(101) Kitajima, N.; Fujisawa, K.; Moro-oka, Y. *Inorg. Chem.* **1990**, *29*, 357.

(102) Kitajima, N.; Katayama, T.; Fujisawa, K.; Moro-oka, Y. *J. Am. Chem. Soc.* **1993**, *115*, 7872.

(103) Nickerson, K. W.; van Holde, K. E. *Comp. Biochem. Physiol.* **1971**, *39D*, 855.

(104) (a) Gaykema, W. P. J.; Hol, W. G. J.; Vereijken, J. M.; Soeter, N. M.; Bak, H. J.; Beintema, J. J. *Nature* **1984**, *309*, 23. (b) Gaykema, W. P. J.; Volbeda, A.; Hol, W. G. J. *J. Mol. Biol.* **1985**, *187*, 255.

(105) (a) Volbeda, A.; Hol, W. G. J. *J. Mol. Biol.* **1989**, *206*, 531. (b) Volbeda, A.; Hol, W. G. J. *J. Mol. Biol.* **1989**, *209*, 249.

(106) Himmelwright, R. S.; Eickman, N. C.; LuBein, C. D.; Solomon, E. I. *J. Am. Chem. Soc.* **1980**, *102*, 5378.

(107) Pate, J.; Thamann, T. J.; Solomon, E. I. *Spectrochim. Acta* **1986**, *42A*, 313.

(108) Solomon, E. I. *Metal Clusters in Proteins*; ACS Symposium Series 372, Que, L., Jr., Ed.; American Chemical Society: Washington DC, 1988; p 116.

(109) Turzek, F.; Solomon, E. I. *Inorg. Chem.* **1993**, *32*, 2850.

(110) Pate, J. E.; Ross, P. K.; Thamann, T. J.; Reed, C. A.; Karlin, K. D.; Sorrell, T. N.; Solomon, E. I. *J. Am. Chem. Soc.* **1989**, *111*, 5198.

(111) Tyeklar, Z.; Karlin, K. D. *Acc. Chem. Res.* **1989**, *22*, 241.

(112) Kitajima, N.; Moro-oka, Y. *J. Chem. Soc., Dalton Trans.* **1993**, 2665.

(113) Kitajima, N. *Bioinorganic Chemistry of Copper*; Karlin, K. D., Tyeklar, Z., Eds.; Chapman & Hall: New York, 1993; p 251.

(114) Hazes, B.; Magnus, K. A.; Bonaventura, C.; Bonaventura, J.; Dauter, Z.; Kalk, K. H.; Hol, W. G. J. *Protein Sci.* **1993**, *2*, 597.

(115) Magnus, K. A.; Ton-That, H.; Carpenter, J. E. *Bioinorganic Chemistry of Copper*; Karlin, K. D., Tyeklar, Z., Eds.; Chapman & Hall: New York, 1993; p 143.

(116) Kitajima, N.; Fujisawa, K.; Hikichi, S.; Moro-oka, Y. *J. Am. Chem. Soc.* **1993**, *115*, 7874.

(117) Pandey, G.; Muralikrishna, C.; Bhalerao, U. T. *Tetrahedron Lett.* **1990**, *31*, 3771.

(118) Kitajima N.; et al. Manuscript in preparation.

(119) (a) James, S. M.; Mu, D.; Wemmer, D.; Smith, A. J.; Kaur, S.; Maltby, D.; Burlingame, A. L.; Klinman, J. P. *Science* **1990**, *248*, 981. (b) Mu, D.; Janes, S. M.; Smith, A. J.; Brown, D. E.; Dooley, D. M.; Klinman, J. P. *J. Biol. Chem.* **1992**, *267*, 7979. (c) Dooley, D. M.; McGuirl, M. A.; Brown, D. E.; Turowski, P. N.; McIntire, W. S.; Knowles, P. F. *Nature* **1991**, *349*, 262.

(120) Ito, N.; Phillips, S. E. V.; Stevens, C.; Ogel, Z. B.; McPherson, M. J.; Keen, J. N.; Yadav, K. D. S.; Knowles, P. F. *Nature* **1991**, *350*, 87.

(121) Chan, S. I.; Nguyen, H.-H. T.; Shiemke, A. K.; Lidstrom, M. E. *Bioinorganic Chemistry of Copper*; Karlin, K. D., Tyeklar, Z., Eds.; Chapman & Hall: New York, 1993; pp 184.

(122) (a) Kau, L.-S.; Spira-Solomon, D. J.; Penner-Hahn, J. E.; Hodgson, K. O.; Solomon, E. I. *J. Am. Chem. Soc.* **1987**, *109*, 6433. (b) Spira-Solomon, E. I. *J. Am. Chem. Soc.* **1987**, *109*, 6421. (c) Cole, J. L.; Ballou, D. P.; Solomon, E. I. *J. Am. Chem. Soc.* **1991**, *113*, 8544.

(123) (a) Messerschmidt, A.; Rossi, A.; Ladenstein, R.; Huber, R.; Bolognesi, M.; Gatti, G.; Marchesini, A.; Petruzzelli, R.; Finazzi-Agro, A. *J. Mol. Biol.* **1989**, *206*, 513. (b) Messerschmidt, A.; Landenstein, R.; Huber, R.; Bolognesi, M.; Avigliano, L.; Petruzzelli, R.; Rossi, A.; Finazzi-Agro, J. *Mol. Biol.* **1992**, *224*, 179.

(124) (a) Malmström, B. G. *Chem. Rev.* **1990**, *90*, 1247. (b) Babcock, G. T.; Wikström, M. *Nature* **1992**, *356*, 301.

(125) (a) Powers, L.; Chance, Y.; Ching, Y.; Angiolillo, P. *Biophys. J.* **1981**, *34*, 465. (b) Bruvig, G. W.; Stevens, T. H.; Chan, S. I. *Biochemistry* **1980**, *19*, 5275.

(126) (a) Ogura, T.; Takahashi, S.; Shinzawa-Itoh, K.; Yoshikawa, S.; Kitagawa, T. *J. Am. Chem. Soc.* **1990**, *112*, 5630. (b) Ogura, T.; Takahashi, S.; Shinzawa-Itoh, K.; Yoshikawa, S.; Kitagawa, T. *J. Am. Chem. Soc.* **1991**, *64*, 2901.

(127) (a) Nanthankumar, A.; Nasir, M. S.; Karlin, K. D. *J. Am. Chem. Soc.* **1992**, *114*, 6564. (b) Nanthakumar, A.; Fox, S.; Nasir, S. M.; Ravi, N.; Huynh, B. H.; Orosz, R. D.; Day, E. P.; Hagen, K. S.; Karlin, K. D. *Proceedings of the 5th International Symposium on the Activation of Dioxygen and Homogeneous Catalytic Oxidation*; Martell, A. E., Sawyer, D. T., Barton, D. H. R., Eds.; Plenum Press: New York, 1993. (c) Nanthakumar, A.; Fox, S.; Murthy, N. N.; Karlin, K. D.; Ravi, N.; Huynh, B. H.; Orosz, R. D.; Day, E. P.; Hagen, K. S.; Blackburn, N. J. *J. Am. Chem. Soc.* **1993**, *115*, 8513.

(128) Lee, S. C.; Holm, R. H. *J. Am. Chem. Soc.* **1993**, *115*, 5833.

(129) (a) Fridovich, I. *Acc. Chem. Res.* **1982**, *15*, 200. (b) Valentine, J. S.; Pantoliano, M. W. *Copper Proteins*; Spiro, T. G., Ed.; Wiley: New York, 1981; p 291.